

Testing the efficiency of different improvement programs

Sergio Caracciolo and Andrea Montanari
Scuola Normale Superiore and INFN – Sezione di Pisa
I-56100 Pisa, ITALIA
Internet: sergio.caracciolo@sns.it, montanar@cibs.sns.it

Andrea Pelissetto
Dipartimento di Fisica and INFN – Sezione di Roma I
Università degli Studi di Roma “La Sapienza”
I-00185 Roma, ITALIA
Internet: pelisset@ibmth.df.unipi.it

October 14, 2018

Abstract

We study the finite-size behaviour of a tree-level on-shell improved action for the N -vector model. We present numerical results for $N = 3$ and analytic results in the large- N limit for the mass gap. We also report a perturbative computation at one loop of the mass gap for states of spatial momentum p . We present a detailed comparison of the behaviour of this action with that of other formulations, including the perfect action, and a critical discussion of the different approaches to the problem of action improvement.

1 Introduction

Lattice simulations are at present the most effective method to investigate non-perturbative properties of field theories like QCD. By necessity Monte Carlo simulations are performed on finite lattices and at finite values of the correlation length. It is therefore of utmost importance to understand the systematic effects due to scaling corrections.

In the last years a lot of work has been devoted to invent lattice models that have small scaling corrections so that continuum results can be obtained on small lattices and thus with a limited use of computer time.

This program was started by Symanzik [1] who put up a systematic method to improve asymptotically free theories using perturbation theory. Soon after, Lüscher and Weisz noticed that simpler actions could be used if one was only interested in on-shell quantities [2]. A different approach is the *perfect-action* program in which improved actions are determined as fixed points of renormalization-group transformations [3–9]. By definition classically perfect actions do not show any lattice effect at tree level. In the standard language they are Symanzik tree-level on-shell improved to all orders of a [10].

Recently the improvement program has been implemented non-perturbatively for the fermionic action [11–14]. This represents an important step forward. Indeed actions that are improved to a finite number of loops have scaling corrections of order $O(a \log^p a)$, or, in the statistical mechanics language, of order $O(\xi^{-1} \log^p \xi)$, where ξ is the correlation length. On the other hand non-perturbatively improved actions should have corrections of order $O(\xi^{-2} \log^q \xi)$. It must be noted however that improvement comes with a price. Improved actions are more complicated than unimproved ones. Thus to understand the practical relevance of any improvement one should also consider the additional cost in the simulations.

In this paper we will study the two-dimensional N -vector model. This theory provides the simplest example for the realization of a nonabelian global symmetry. Its two-dimensional version has been extensively studied because it shares with four-dimensional gauge theories the property of being asymptotically free in the weak-coupling perturbative expansion [15–17]. This picture predicts a nonperturbative generation of a mass gap that controls the exponential decay of the correlation functions at large distance.

Besides perturbation theory, the two-dimensional N -vector model can be studied using different techniques. It can be solved in the $N = \infty$ limit [18, 19] and $1/N$ corrections can be systematically calculated [20–22]. An exact S -matrix can be computed [23, 24] and, using the thermodynamic Bethe ansatz, the exact mass gap of the theory in the limit $\beta \rightarrow \infty$ has been obtained [25, 26]. The model has also been the object of extensive numerical work [27–32] mainly devoted to checking the correctness of the perturbative predictions [33–36].

We will consider the action that has been proposed in Ref. [37]. It is on-shell tree-level improved and satisfies reflection positivity so that a positive transfer matrix can be defined. Moreover we will show here that this action can be efficiently simulated: indeed one can use a Wolff algorithm [38–41] with unfrustrated embedded Ising model. Therefore no critical slowing down is expected. This is at variance with the standard Symanzik tree-level action. Indeed, also in this case one can define a cluster algorithm [42]. However the embedded Ising model is frustrated and therefore critical slowing down is still present.

The purpose of this work is twofold. First of all we want to understand quantitatively the effect of tree-level improvement. Indeed it is not obvious *a priori* that the idea is effective since the corrections to scaling are simply reduced a logarithm of a . As we shall see from our numerical results for $N = 3$ and our analytic expressions in the large- N limit, tree-level improvement effectively works: indeed one finds “naturally” — i.e. without any additional tuning of the parameters — a reduction of the scaling corrections by approximately a factor of two. The second purpose of this work was to understand the results of Ref. [3] for the perfect action which shows, for a particular value of the parameter κ that parametrizes the renormalization-group transformations, a dramatic improvement with respect to the standard action. The on-shell action that is considered in this paper differs from the action of Ref. [3] by terms of order a^4 and it shares the property of being extremely local. We thus wanted to understand if the results of Ref. [3] depended only on the improvement and on the locality of the action. The answer is clearly negative, since the on-shell action we study has much larger corrections. At this point the question that arises naturally is whether the exceptionally good behaviour is related to the fact that the action is a classical fixed point of a renormalization-group transformation. Extending the perturbative calculation of Ref. [10] we will see that this interpretation is unlikely. Indeed with a different choice of the parameter κ one can define perfect actions that are local but that are not expected to have such a good behaviour.

In this paper we will investigate the corrections to finite-size scaling (FSS) for various models that are introduced in Sect. 2. A discussion of the FSS corrections in the large- N limit is presented in Sect. 3. We will show here that tree-level improvement reduces the corrections to scaling from $\log L/L^2$ to $1/L^2$. Sect. 4 presents our algorithm and Monte Carlo results. Finally in Sect. 5 we present our conclusions and compare our results with those obtained with other types of action. App. A presents the details of the analytic calculation of the FSS functions for the on-shell action in the large- N limit, App. B the analytic computation at one loop of the mass gap for non-vanishing spatial momentum while in App. C we give some details of our calculations with the perfect action.

Preliminary results of this work have been presented at the Lattice 97 conference [43].

2 The models

In this work we will study in detail the FSS properties of the tree-level on-shell improved action proposed in Ref. [37]:

$$S^{onshell}(\boldsymbol{\sigma}) = \sum_x \left[\frac{2}{3} \sum_{\mu} (\boldsymbol{\sigma}_x \cdot \boldsymbol{\sigma}_{x+\mu}) + \frac{1}{6} \sum_d (\boldsymbol{\sigma}_x \cdot \boldsymbol{\sigma}_{x+d}) - \frac{1}{24} \sum_{s_1=\pm 1} \sum_{s_2=\pm 1} (\boldsymbol{\sigma}_x \cdot \boldsymbol{\sigma}_{x+s_1\hat{1}} + \boldsymbol{\sigma}_x \cdot \boldsymbol{\sigma}_{x+s_2\hat{2}} - 2)^2 \right], \quad (2.1)$$

where d runs over the diagonal vectors $(1, \pm 1)$, while in the last term $\hat{1}$ and $\hat{2}$ are the unit vectors along the x - and y -axis respectively. It was shown in Ref. [37] that the action (2.1) is reflection-positive and tree-level on-shell improved. In the formal continuum limit

we have

$$S^{onshell}(\boldsymbol{\sigma}) \approx \int d^2x \left[\frac{1}{2}(\boldsymbol{\sigma} \cdot \square \boldsymbol{\sigma}) + \frac{\alpha_2 a^2}{2}(\boldsymbol{\sigma} \cdot \square^2 \boldsymbol{\sigma} - (\boldsymbol{\sigma} \cdot \square \boldsymbol{\sigma})^2) + O(a^4) \right] \quad (2.2)$$

where $\square = \sum_{\mu} \partial_{\mu}^2$ and $\alpha_2 = -\frac{1}{12}$.

We will study the FSS corrections for this action and we will compare these results with those obtained for other actions that have been extensively studied in the literature:

- the *standard action*

$$S^{std}(\boldsymbol{\sigma}) = \sum_{x,\mu} \boldsymbol{\sigma}_x \cdot \boldsymbol{\sigma}_{x+\mu} \quad (2.3)$$

whose FSS behaviour has been extensively studied in Refs. [29, 44, 45];

- the *Symanzik action* [1]

$$S^{sym}(\boldsymbol{\sigma}) = \sum_{x,\mu} \left(\frac{4}{3} \boldsymbol{\sigma}_x \cdot \boldsymbol{\sigma}_{x+\mu} - \frac{1}{12} \boldsymbol{\sigma}_x \cdot \boldsymbol{\sigma}_{x+2\mu} \right) \quad (2.4)$$

which is designed to cancel $O(a^2)$ lattice artifacts in tree-level Green functions [1];

- the *diagonal action* [46]

$$S^{diag}(\boldsymbol{\sigma}) = \sum_{x,d} \left(\frac{2}{3} \boldsymbol{\sigma}_x \cdot \boldsymbol{\sigma}_{x+\mu} + \frac{1}{6} \boldsymbol{\sigma}_x \cdot \boldsymbol{\sigma}_{x+d} \right) \quad (2.5)$$

whose one-particle spectrum has no $O(a^2)$ artifacts at tree level but that is not on-shell improved. For instance the four-point function shows $O(a^2)$ corrections even on-shell.

- the classically perfect action [3, 4] that is defined as the fixed point of a class of renormalization-group transformations for $\beta = \infty$. The two-spin part is given by

$$S^{perf,2spin}(\boldsymbol{\sigma}) = \sum_{x,y} w(x-y) \boldsymbol{\sigma}_x \cdot \boldsymbol{\sigma}_y, \quad (2.6)$$

where $w(x)$ is the so-called *perfect laplacian* [47]. Its Fourier transform is given by

$$\frac{1}{w(q)} = \frac{1}{3\kappa} + \sum_{l_1, l_2 = -\infty}^{\infty} \frac{1}{(q_1 + 2\pi l_1)^2 + (q_2 + 2\pi l_2)^2} \frac{\widehat{q}_1^2 \widehat{q}_2^2}{(q_1 + 2\pi l_1)^2 (q_2 + 2\pi l_2)^2}, \quad (2.7)$$

where κ is a parameter that characterizes the renormalization-group transformation. The four-spin coupling — and also higher order couplings — cannot be computed in closed form. In App. C we give some details on our determination of the four-spin term for various values of κ . The formal continuum limit of the perfect action is given by Eq. (2.2) with $\alpha_2 = (\kappa - 4)/(12\kappa)$. Notice that the perfect action with $\kappa = 2$ and the on-shell action (2.1) are, at tree level, equivalent also off-shell up to terms of order a^4 .

3 FSS functions in the large- N limit

In this section we will discuss the relation between improvement and finite-size scaling in the large- N limit extending the discussion of Ref. [48]. We will consider an $L \times T$ square lattice and we will generalize the action (2.1) considering

$$S[\boldsymbol{\sigma}] = N \sum_{x,y} J(x-y) \boldsymbol{\sigma}_x \cdot \boldsymbol{\sigma}_y + \frac{\alpha_3 N}{2} \sum_{x,y,z} K(x-y) K(x-z) (\boldsymbol{\sigma}_x \cdot \boldsymbol{\sigma}_y) (\boldsymbol{\sigma}_x \cdot \boldsymbol{\sigma}_z), \quad (3.1)$$

where

$$\hat{K}(p) \equiv \sum_x K(x) e^{-ipx} = p^2 + O(p^4), \quad (3.2)$$

$$\hat{J}(p) \equiv \sum_x J(x) e^{-ipx} \equiv \hat{J}(0) - \frac{1}{2} w(p), \quad (3.3)$$

$$w(p) = \hat{p}^2 + \alpha_1 \sum_{\mu} \hat{p}_{\mu}^4 + \alpha_2 (\hat{p}^2)^2 + O(p^6). \quad (3.4)$$

Here $\hat{p}^2 \equiv \sum_{\mu} \hat{p}_{\mu}^2 \equiv \sum_{\mu} (2 \sin(p_{\mu}/2))^2$.

We will assume, as usual, that all the couplings respect the symmetry of the lattice and that $w(p)$ vanishes only for $p = 0$ in the Brillouin zone. Moreover we require the action to be ferromagnetic, that is to have a unique maximum corresponding to the ordered configuration. The general class of actions (3.1) was studied in Ref. [37] where it was shown that $S[\boldsymbol{\sigma}]$ is tree-level on-shell improved if $\alpha_1 = 1/12$ and $\alpha_2 = \alpha_3$.

In the large- N limit the model can be solved using a standard Lagrange-multiplier technique. One introduces two parameters $m_{L,T}$ and $\omega_{L,T}$ related to β by the gap equations¹:

$$\beta(1 + \omega_{L,T}) = \frac{1}{LT} \sum_p \frac{1}{\hat{w}(p; \omega_{L,T}) + m_{L,T}^2}, \quad (3.5)$$

$$-\frac{\beta}{2\alpha_3} (1 + \omega_{L,T}) \omega_{L,T} = \frac{1}{LT} \sum_p \frac{\hat{K}(p)}{\hat{w}(p; \omega_{L,T}) + m_{L,T}^2}, \quad (3.6)$$

where

$$\hat{w}(p; \omega) \equiv \frac{w(p) + \omega \hat{K}(p)}{1 + \omega}. \quad (3.7)$$

The two-point function is simply given by:

$$\langle \boldsymbol{\sigma}_x \cdot \boldsymbol{\sigma}_y \rangle = \frac{1}{\beta(1 + \omega_{L,T})} \frac{1}{LT} \sum_p \frac{e^{ip(x-y)}}{\hat{w}(p; \omega_{L,T}) + m_{L,T}^2}. \quad (3.8)$$

¹We should remark that for some choices of $K(x)$ and $J(x)$ these equations may not be correct for all values of β (see for instance the exact solution of the mixed $O(N) - RP^{N-1}$ models of Ref. [49]). However under our hypotheses they should always describe the theory for sufficiently large values of β . This is sufficient for our analysis since we are only interested in the critical limit $\beta \rightarrow \infty$.

In Appendix A we present an analytic computation of the FSS curves and of their leading correction. For the mass gap $\mu(L, \beta)$ defined on a strip $L \times \infty$, in the limit $\beta \rightarrow \infty$, $L \rightarrow \infty$, with $\mu(L, \beta)L \equiv x$ fixed, we find

$$\left(\frac{\mu(\infty, \beta)}{\mu(L, \beta)}\right)^2 = f_\mu(x) \left(1 + \frac{\Delta_\mu(x; L)}{L^2} + O(L^{-4} \log^2 L)\right). \quad (3.9)$$

The function $f_\mu(x)$ is the FSS function and it was already computed by Lüscher [50]:

$$f_\mu(x) = \exp \left[-4 \sum_{n=1}^{\infty} K_0(nx) \right] = \frac{16\pi^2 e^{-2\gamma_E}}{x^2} \exp \left[-\frac{2\pi}{x} \right] (1 + O(x)). \quad (3.10)$$

The function $\Delta_\mu(x; L)$ is the leading correction to FSS. For $L \rightarrow \infty$ keeping x fixed, it behaves as $\log L$ and it has a regular expansion in powers of $1/\log L$ of the form

$$\Delta_\mu(x; L) = \sum_{q=-1}^{\infty} \delta_{\mu,q}(x) (\log L)^{-q}. \quad (3.11)$$

The leading term is given by

$$\delta_{\mu,-1}(x) = \frac{x^2}{4} (1 - f_\mu(x)) (1 - 12\alpha_1 - 16\alpha_2 + 16\alpha_3). \quad (3.12)$$

It vanishes for tree-level improved actions. Thus improvement reduces the corrections to scaling from $\log L/L^2$ to $1/L^2$. Generically, the next coefficient $\delta_{\mu,0}(x)$ does not vanish for tree-level improved actions. However one can choose $K(x)$ and $J(x)$ in order to have $\delta_{\mu,0}(x) = 0$ (see Appendix A). In other words, with an appropriate choice of these two functions it is possible to improve the action to one-loop order. One can verify that it is not possible to obtain $\delta_{\mu,1}(x) = 0$ for $\alpha_3 \neq 0$. In this case, actions of the form (3.1) cannot be two-loop on-shell improved. This is not unexpected since, six-spin couplings are needed for two-loop improvement. If $\alpha_3 = 0$ the situation is simpler. Indeed in this case, once the action is one-loop improved, it is automatically improved to all orders of perturbation theory [37]. This is however an accident of the large- N limit and it is not true for finite values of N .

Since tree-level improvement reduces FSS corrections only by a logarithm of L , one could be skeptical on the effectiveness of the idea. We have therefore compared the FSS scaling corrections for various actions. In Table 1 we report $\mu(\infty, \beta)/\mu(L, \beta)$ for various values of L for $x = 2$ for the on-shell action (2.1), as well as for the actions (2.3) and (2.4). It is clear that tree-level improved actions show much smaller corrections. For the purpose of future comparison we consider also the quantity

$$R(L, x) \equiv 2L\mu(2L, \beta). \quad (3.13)$$

It is easy to convince oneself that in the FSS limit $R(L, x)$ assumes a finite value $R(\infty, x)$ with corrections of order $\log L/L^2$. In Fig. 1 we show $R(L, x)$ for $x = 1.0595$ for various actions. Also here it is evident that improved actions show smaller corrections to scaling.

L	S^{std}	S^{sym}	$S^{onshell}$
4	0.79362345	0.78565020	0.78324283
6	0.78640181	0.78100623	0.78024309
8	0.78290367	0.77913556	0.77884796
10	0.78099463	0.77822405	0.77808048
16	0.77857473	0.77720115	0.77717924
20	0.77792482	0.77696043	0.77697663
32	0.77714433	0.77669433	0.77669910
∞	0.77652331	0.77652331	0.77652331

Table 1: $\mu(\infty, \beta)/\mu(L, \beta)$ for $x = 2$ for different lattice actions.

Let us now discuss the validity of the expansion (3.9). First of all the expansion is not uniform in x : the error increases as $x \rightarrow \infty$. This fact can be checked analytically from the exact expressions of App. A. Its origin is easy to understand. In order to have FSS one should work at values of β such that the correlation length is much larger than one lattice spacing, i.e. $\mu(L) \ll 1$. This means that the expansion (3.9) makes sense only for $x/L \ll 1$.

We want finally to discuss the connection between the FSS limit for $x \rightarrow 0$ and perturbation theory (PT). The PT limit corresponds to $\beta \rightarrow \infty$ with L fixed. For instance for $\mu(L)$ one obtains

$$x \equiv \mu(L)L = \frac{1}{\beta} \sum_{n=0}^{\infty} \frac{a_n(L)}{\beta^n}, \quad (3.14)$$

where $a_n(L)$ has an expansion of the form

$$a_n(L) = \sum_{k=0}^n a_{nk}^{(0)} \log^k L + \frac{1}{L^2} \sum_{k=0}^n a_{nk}^{(1)} \log^k L + O(L^{-4}). \quad (3.15)$$

This expansion can be inverted to give

$$\beta = \frac{1}{x} \sum_{n=0}^{\infty} b_n(L) x^n, \quad (3.16)$$

where the coefficient $b_n(L)$ have an expansion of the form (3.15). To obtain the FSS curve one can then use the asymptotic freedom prediction

$$\mu(\infty) = A \left(\frac{2\pi N\beta}{N-2} \right)^{\frac{1}{N-2}} \exp \left(-\frac{2\pi N\beta}{N-2} \right) \left(1 + \sum_{n=1}^{\infty} \frac{c_n}{\beta^n} \right), \quad (3.17)$$

and substitute the expansion of β in terms of x . In this way one computes $\mu(\infty)/\mu(L)$. The leading term for $L \rightarrow \infty$ is L -independent and correctly reproduces the expansion of

the exact result (3.10). One can also compute the first correction in powers of $1/L^2$. In this way one obtains the expansion of $\Delta_\mu(x; L)$ for L fixed in the limit $x \rightarrow 0$:

$$\Delta_\mu(x; L) = \sum_n P_n(\log L)x^n, \quad (3.18)$$

where $P_n(x)$ is a degree- n polynomial. Clearly this expansion is incorrect for $L \rightarrow \infty$, although, for finite small x , it gives a reasonable approximation as long as $L \ll L_{max}(x) \approx e^{\pi/x}$. In the opposite limit $L \gg L_{max}(x)$, the correct expansion is given by Eq. (3.11). This result reflects the fact that the PT limit $\beta \rightarrow \infty$ at fixed L (equivalent to $x \rightarrow 0$ at fixed L), followed by $L \rightarrow \infty$ does not commute with the FSS limit followed by $x \rightarrow 0$, except for the leading term [48].

Numerically PT calculations of the corrections to FSS can still be useful, at least if one is able to compute enough terms. We have considered for instance $R(L, x)$ that admits an expansion of the form

$$R(L, x) = R_0(x) + \frac{1}{L^2}R_1(x; \log L) + \dots \quad (3.19)$$

where $R_0(x) \equiv R(\infty, x)$ is the FSS function. For the on-shell action (2.1) we have up to three-loops

$$R_1(x; \log L) = -0.0251916x^3 + (0.0321612 + 0.008018747 \log L)x^4 + O(x^5). \quad (3.20)$$

Because the action is improved there is no x^2 (one-loop) term. Consider now $\Delta R(L, x) \equiv R(L, x) - R_0(x)$. For $x = 1.0595$ and $L = 8, 64$ we obtain the estimates

$$\begin{aligned} \Delta R(8, 1.0595) &= 0 \text{ (1 loop); } -0.4681 \cdot 10^{-3} \text{ (2 loops); } 0.4934 \cdot 10^{-3} \text{ (3 loops),} \\ \Delta R(64, 1.0595) &= 0 \text{ (1 loop); } -0.7314 \cdot 10^{-5} \text{ (2 loops); } 0.1284 \cdot 10^{-4} \text{ (3 loops).} \end{aligned}$$

This should be compared with the exact results $0.751 \cdot 10^{-3}$ for $L = 8$ and $0.147 \cdot 10^{-4}$ for $L = 64$. The three-loop result is reasonably close to the exact value while the two-loop approximation gives a grossly inexact guess (it has even the wrong sign) of the exact result.

4 Monte Carlo results

As we have seen in the previous section tree-level improvement changes the correction to FSS by a $\log L$. A priori this appears to be a very small improvement. However at $N = \infty$ the actions (2.1) and (2.4) show a much better behaviour with respect to the standard action (2.3). We decided to check if this is true also for $N = 3$, comparing our data for the mass gap with the simulation results of Ref. [44] for the standard action and of Ref. [3] for the perfect action.

We have used in our simulation the Wolff algorithm [38–41] with standard Swendsen-Wang updatings [51, 52]. The idea is the following: given a spin configuration $\{\sigma_x\}$, one chooses randomly a unit vector \mathbf{r} and defines Ising variables ϵ_x rewriting

$$\sigma_x = \epsilon_x \sigma_{\parallel x} + \sigma_{\perp x}, \quad (4.1)$$

where $\sigma_{\parallel x}$ and $\sigma_{\perp x}$ are the components of σ_x respectively parallel and perpendicular to \mathbf{r} . Eq. (4.1) defines an effective action $S^{eff}(\{\epsilon\})$ for the embedded Ising variables. A simplifying feature of our action (2.1) is that the effective action $S^{eff}(\{\epsilon\})$ contains only two-spin Ising couplings and therefore it can be updated using a standard cluster algorithm. We can indeed rewrite the action (2.1) as

$$S^{onshell} = \sum_x \left\{ \frac{4}{3} \left(\begin{array}{c} \bullet \\ \bullet \end{array} \right) + \frac{1}{6} \left(\begin{array}{c} \bullet \\ \diagdown \\ \bullet \end{array} + \begin{array}{c} \bullet \\ \diagup \\ \bullet \end{array} \right) + \right. \\ \left. - \frac{1}{24} \left[\left(\begin{array}{c} \bullet \\ \bullet \\ \bullet \end{array} \right) + \left(\begin{array}{c} \bullet \\ \bullet \\ \bullet \end{array} \right) + 2 \left(\begin{array}{c} \bullet \\ \bullet \\ \bullet \end{array} \right) + \dots \right] \right\}$$

The Wolff embedding acts on these couplings as follows:

$$\begin{array}{c} x \qquad y \\ \bullet \text{---} \bullet \end{array} = \sigma_x \cdot \sigma_y \rightarrow \epsilon_x \epsilon_y \sigma_{\parallel x} \cdot \sigma_{\parallel y} \quad (4.2)$$

$$\begin{array}{c} x \qquad y \\ \bullet \text{====} \bullet \end{array} = (\sigma_x \cdot \sigma_y)^2 \rightarrow 2\epsilon_x \epsilon_y \sigma_{\parallel x} \cdot \sigma_{\parallel y} \sigma_{\perp x} \cdot \sigma_{\perp y} \quad (4.3)$$

$$\begin{array}{c} y \qquad z \\ \bullet \text{---} \bullet \\ | \\ x \\ \bullet \end{array} = (\sigma_y \cdot \sigma_x)(\sigma_y \cdot \sigma_z) \rightarrow \epsilon_x \epsilon_z \sigma_{\parallel x} \cdot \sigma_{\parallel y} \sigma_{\parallel y} \cdot \sigma_{\parallel z} \\ + \epsilon_y \epsilon_z \sigma_{\parallel y} \cdot \sigma_{\parallel z} \sigma_{\perp x} \cdot \sigma_{\perp y} \\ + \epsilon_y \epsilon_x \sigma_{\parallel y} \cdot \sigma_{\parallel x} \sigma_{\perp z} \cdot \sigma_{\perp y} \quad (4.4)$$

The embedded action becomes

$$S^{eff}(\{\epsilon\}) = \sum_x \left[\sum_{\mu} J_{x\mu}^{(1)} \epsilon_x \epsilon_{x+\mu} + \sum_d J_{xd}^{(2)} \epsilon_x \epsilon_{x+d} \right], \quad (4.5)$$

where d are the diagonal vectors $(1, \pm 1)$. The couplings are defined by

$$J_{x\mu}^{(1)} = (\sigma_{\parallel x} \cdot \sigma_{\parallel x+\mu}) \left[\frac{4}{3} - \frac{1}{3} \sigma_{\perp x} \cdot \sigma_{\perp x+\mu} - \frac{1}{12} \sigma_{\perp x} \cdot \sigma_{\perp x+\nu} - \frac{1}{12} \sigma_{\perp x} \cdot \sigma_{\perp x-\nu} - \right. \\ \left. \frac{1}{12} \sigma_{\perp x} \cdot \sigma_{\perp x+\nu+\mu} - \frac{1}{12} \sigma_{\perp x} \cdot \sigma_{\perp x-\nu+\mu} \right], \quad (4.6)$$

$$J_{xd}^{(2)} = \frac{1}{6} (\sigma_{\parallel x} \cdot \sigma_{\parallel x+d}) \left[1 - \frac{1}{2} \sigma_{\parallel x+\hat{1}}^2 - \frac{1}{2} \sigma_{\parallel x+d-\hat{1}}^2 \right], \quad (4.7)$$

where, in the first definition, ν is a unit vector orthogonal to μ . It is easy to see that the embedded Ising model is not frustrated. Indeed if we redefine the Ising variables as

$$\epsilon'_x = \epsilon_x \text{sign}(\sigma \cdot \mathbf{r}) \quad (4.8)$$

we obtain a new effective action of the type (4.5) with $J_{x\mu}^{(1)} \geq 0$, $J_{xd}^{(2)} \geq 0$. Therefore we expect the algorithm not to show any critical slowing down [41].

The purpose of our simulation was the determination of the FSS function $R(L, x)$ defined in Eq. (3.13) for $x \equiv \mu(L, \beta)L = 1.0595$ for a strip $L \times \infty$ with periodic boundary conditions (pbc) in the spatial direction. This is indeed the value of x for which results are available for the standard [44] and for the perfect action [3]. Given L , in order to compute $R(L, x)$, we have first determined $\tilde{\beta}$ such that $\mu(\tilde{\beta}, L) = 1.0595$. This has been obtained performing a Monte Carlo simulation at a nearby value β_{run} of β , and appropriately reweighting the correlation functions. Analogously $\mu(\tilde{\beta}, 2L)$ has been determined from a Monte Carlo simulation at a nearby value of β and then applying the appropriate reweighting. Since we use small lattices, the reweighting technique works very well and it does not increase significantly the error bars.

Since we wanted to determine the mass gap with high precision we paid particular attention to systematic effects. Most of the simulations were done on lattices $L \times T$ with pbc and $T = 10L$. We computed the correlation function

$$G(t) = \frac{1}{TL^2} \sum_{x_1, x_2, y} \langle \sigma_{x_1, y} \cdot \sigma_{x_2, y+t} \rangle, \quad (4.9)$$

and extracted the mass gap assuming

$$G(t) \sim \cosh m \left(\frac{T}{2} - t \right) \quad (4.10)$$

for $L \lesssim t \lesssim T/2$. To check for possible systematic deviations we also performed two simulations with “cold wall” boundary conditions: in this case the spins at one temporal boundary ($t = 0$) were fixed in one direction σ^{wall} while we used free boundary conditions on the other side. Of course, in the spatial direction we still used pbc. In this case the mass gap was extracted from

$$G(t) = \sum_x \langle \sigma^{wall} \cdot \sigma_{t, x} \rangle \quad (4.11)$$

that is expected to behave as e^{-mt} for t large. This type of boundary conditions automatically projects out the excited modes that have energy

$$E_l(\beta, L) - E_0(\beta, L) = \frac{1}{2\beta L} l(l+1) + O(\beta^{-2}), \quad (4.12)$$

and therefore reduces the systematic errors. However it has a disadvantage for our purposes: with respect to pbc, much longer simulations are required to obtain the mass gap with the same precision. We have performed two runs at $L = 5, 10$ with “cold wall” boundary conditions and we have not observed any systematic difference with respect to the runs with pbc (see Table 2). Therefore we believe that our results have a systematic error that is smaller than the statistical one.

The results of our simulations are reported in Table 2. The total simulation took approximately 5 months of CPU-time on a SGI Origin2000.

These results are shown in Fig. 2 together with the previously obtained ones referring to the *standard* [44] and *perfect* [3] actions. Clearly the on-shell action is better than the standard action. However its behaviour is worse than that of the perfect action which shows no scaling corrections even for $L = 5$.

$L \times T$	b.c.	β_{run}	$\tilde{\beta}$	$\mu(\tilde{\beta})L$	N_{stat}	$T_{CPU}(\text{ms})$
5×30	periodic	1.212	1.21045 ± 0.00025	*	$15 \cdot 10^6$	11/4.5
10×100	periodic	1.212	*	1.2780 ± 0.0019	$3.75 \cdot 10^6$	78/30
5×50	cold wall	1.212	1.2104 ± 0.0004	*	$84 \cdot 10^6$	11/8
10×60	cold wall	1.212	*	1.278 ± 0.002	$175 \cdot 10^6$	25/18
7×70	periodic	1.260	1.2691 ± 0.0004	*	$21.2 \cdot 10^6$	38/15
14×140	periodic	1.260	*	1.2782 ± 0.0009	$11 \cdot 10^6$	180/60
10×100	periodic	1.340	1.32835 ± 0.00018	*	$16.2 \cdot 10^6$	78/30
20×200	periodic	1.330	*	1.2738 ± 0.0007	$7.2 \cdot 10^6$	420/122

Table 2: Monte Carlo results. β_{run} is the value of β at which the Monte Carlo simulation was done, $\tilde{\beta}$ is the value of β such that $\mu(\tilde{\beta}, L) = 1.0595$. N_{stat} is the number of iterations of a Wolff algorithm with standard Swendsen-Wang updatings. T_{CPU} is the CPU time in ms for a iteration on a SGI Origin2000: the first number is the total CPU time spent in our simulation, the second number is the time spent in the updating only, i.e. without measuring the two-point function.

5 Critical discussion

In this paper we have investigated the FSS behaviour of the action (2.1). The main point was to understand, in a model in which high-statistics data can be generated, how effective perturbative improvement is. Our large- N analysis presented in Sect. 3 shows that tree-level improvement effectively reduces the scaling corrections. In this limit, simulations with the standard action on a lattice of volume L^2 would be affected by the same systematic errors of results obtained on a lattice of size of order $L/2$ using the action (2.1) (cf. Table 1 and Fig. 1). For $N = 3$ our numerical data show a similar effect. Therefore, using the tree-level improved action (2.1) one can perform simulations on a lattice that is four times smaller and still obtain the same scaling corrections. Of course, in order to make a fair comparison of the two actions, we should take into account the fact that the action (2.1) is more complicated and therefore one Monte Carlo iteration is slower. For instance, one update with the on-shell action takes 30 ms on a 10×100 lattice (see Table 2), while it takes 11 ms if one uses the standard action. Therefore, the time spent in the updating is reduced only by 20–30%. However it is also important to take into account the time spent in the measurement of the observables. In our simulation we measured the two-point function: the total CPU-time per iteration on 10×100 lattice is 78 ms, which should be compared to 300 ms spent by the standard action on a 20×200 lattice. Using the on-shell action we obtain comparable results for this quantity in 1/4 of the CPU time. Notice that we expect the two-dimensional σ -model to be the case in which Symanzik improvement has the smaller pay-off. Indeed in this case the lattice volume increases only as L^2 , and the algorithm does not have critical slowing down, so that working with large volumes is not so expensive. In QCD the situation would be radically different since in this case the CPU time to produce an independent configuration scales as L^{4+z} with $z \gtrsim 2$. Thus, even a small reduction of the needed values of L , significantly reduces the computer time.

Of course, the skeptical reader may think that the better behaviour of the improved

action is a mere numerical coincidence. After all, we have simply improved the behaviour of the corrections to scaling by $\log L$, which is a very slowly varying function: therefore, it is not even obvious that, for our range of values of L , say $L \approx 16$ –128, an improved action behaves better than the standard one. Indeed it is possible to write down (complicated) actions that are not tree-level improved and yet, for $L \approx 16$ –128, behave better than the action (2.1), and, viceversa, to invent improved actions that, in the same range of values of L , are worse than the standard action. However the relevant question — unfortunately a not well defined one — is whether “simple” local tree-level improved actions behave better as long as L is larger than 1. In order to understand if there is a positive answer, we should study different actions. We have considered the Symanzik tree-level action (2.4). For $N = \infty$ the actions (2.1) and (2.4) behave similarly, and also for $N = 3$ no significant difference is observed [53]. Another tree-level improved action is the perfect action [3]. Also in this case numerical simulations show a better behaviour, see Fig. 2. Tree-level improvement seems really to work.

Let us now compare the various improved actions in more detail. While the theories defined by (2.1) and (2.4) behave similarly, the perfect action is vastly better and indeed it does not show any corrections to scaling (at the level of 1–2%) even for $L = 5$. A possible explanation of this behaviour has been suggested by Hasenfratz and Niedermayer [10]. They show that the classically perfect action used in the simulations reported in Ref. [3] has very small one-loop corrections so that it can be effectively considered one-loop improved. As an indication of how much one-loop improved an action is, they suggested considering the mass gap of states with spatial momentum p in perturbation theory at one loop. The general analytic calculation of this quantity at one loop is reported in App. B. If we define the correlation function

$$G(t, p) = \frac{1}{L} \sum_{x_1, x_2} \langle \sigma_{0, x_1} \cdot \sigma_{t, x_2} \rangle e^{ip \cdot (x_2 - x_1)}, \quad (5.1)$$

and the mass gap $\omega(p)$

$$\omega(p) = - \lim_{|t| \rightarrow \infty} \frac{\log G(t, p)}{|t|}, \quad (5.2)$$

then, we find in perturbation theory

$$\omega(p)L = pL + \frac{1}{2\beta} + \frac{1}{L^2} \widehat{\omega}(pL, \beta) + O(\beta^{-2}, L^{-4}). \quad (5.3)$$

For the various action we obtain:

$$\text{standard} \quad \widehat{\omega}(pL, \beta) = -\frac{1}{12}(pL)^3 + \frac{\pi}{12\beta} pL; \quad (5.4)$$

$$\text{on-shell} \quad \widehat{\omega}(pL, \beta) = -\frac{(pL)^3}{\beta} [0.01604(N-1) + 0.01321]; \quad (5.5)$$

$$\text{Symanzik} \quad \widehat{\omega}(pL, \beta) = -\frac{(pL)^3}{\beta} 0.01237; \quad (5.6)$$

$$\text{perf. } \kappa = 2 \quad \widehat{\omega}(pL, \beta) = -\frac{(pL)^3}{\beta} [a_{pf}(N-1) - 0.0004]. \quad (5.7)$$

We have been unable to estimate the constant a_{pf} precisely, but our results indicate $|a_{pf}| \lesssim 0.0005$. From the estimates of Ref. [10] we would obtain the bound $|a_{pf}| \lesssim 10^{-4}$.

As expected, for tree-level improved actions, there are no β^0 corrections. Considering now the $O(\beta^{-1})$ terms, we see that the perfect action has much smaller corrections compared to the Symanzik and the on-shell one. Therefore, if the good scaling behaviour of the perfect action is related to the fact that it is effectively one-loop improved — in other words, if higher order corrections play little role — our results could have been expected on the basis of the results for the mass gap we reported above. A check of this argument consists in verifying that an action that is exactly one-loop improved and is sufficiently local has the same good scaling behaviour of the perfect action. A simulation is in progress. Of course, at the end of this discussion, the most important question concerning the effectiveness of perfect actions remains unanswered: had we to expect *a priori* that the perfect action has very small one-loop corrections? For $\kappa = +\infty$ the action is exactly one-loop improved, but the couplings are long-range so that this fact is of no practical interest. The interesting question is what happens for those values of κ that correspond to sufficiently local actions. To answer it we have computed the four-spin coupling of the perfect action for various values of κ and correspondingly the correction $\widehat{\omega}(pL, \beta)$. The results for the perturbative coefficients (see Eq. (B.31)) are shown in Fig. 3, where, for each value of κ , we report two points corresponding to two different truncations of the action, corresponding to including respectively 51 and 771 different couplings in the four-spin term of the action (see App. C for details). One immediately sees that the corrections increase strongly as $\kappa \rightarrow 0$, and, for instance for $\kappa = 0.75$, the corrections are of the same order of those of the action (2.1). In other words, the renormalization-group procedure which is the basis of the perfect action approach does not provide naturally actions that are “numerically” improved: there are classically perfect actions that are relatively local and that behave no better than (2.1). In conclusion we do not see any theoretical reason for the exceptionally good behaviour found in Ref. [3]. Indeed it is not a *a priori* obvious — in the sense that it is not built in the approach — that there exists a value of κ such that the action is local and the corrections are small.

Acknowledgments

The numerical computations presented in this paper have been performed at the Computer Center of the Scuola Normale Superiore in Pisa.

A Finite-size scaling in the large- N limit

A.1 Definitions

In this section we will report some definitions and expressions that will be used in our computation of the corrections to FSS.

FSS functions are expressed in terms of the so-called remnant functions [54]. We define

$$G_k(\alpha) = \sum_{n=1}^{\infty} \left[(n^2 + \alpha^2)^{k-1/2} - \sum_{m=0}^k \binom{k-1/2}{m} \alpha^{2m} n^{2k-2m-1} \right], \quad (\text{A.1})$$

$$H_k(\alpha) = \sum_{n=1}^{\infty} \frac{1}{(n^2 + \alpha^2)^{k+1/2}}, \quad (\text{A.2})$$

where $k \geq 0$ (resp. $k \geq 1$) in the first (resp. second) case. Asymptotic expressions and various properties of the remnant functions are reported in Ref. [54] and in Appendix A.1 of Ref. [48].

Our results are expressed in terms of the functions $F_0(z; \rho)$ and $F_1(z; \rho)$. They are defined by the asymptotic expansion of the lattice sum

$$I_{L,T}(m^2) = \frac{1}{LT} \sum_{n_x=0}^{L-1} \sum_{n_y=0}^{T-1} \frac{1}{\hat{p}^2 + z^2/L^2} \quad (\text{A.3})$$

for $L, T \rightarrow \infty$ with z and $\rho = L/T$ fixed. Here $\hat{p}^2 = 4 \sin^2(p_x/2) + 4 \sin^2(p_y/2)$, $p_x = 2\pi n_x/L$, and $p_y = 2\pi n_y/T$. We obtain

$$I_{L,T}(m^2) = \frac{1}{2\pi} \log L + F_0(z; \rho) - \frac{z^2}{16\pi L^2} \log L + \frac{1}{L^2} F_1(z; \rho) + O(L^{-4} \log L). \quad (\text{A.4})$$

Explicit expressions for $F_0(z; \rho)$ and $F_1(z; \rho)$ for arbitrary ρ are reported in App. B of Ref. [48]. Here we report them only for the strip case, i.e. for $\rho = \infty$. We have

$$F_0(z; \infty) = \frac{1}{2z} + \frac{1}{2\pi} \left(\gamma_E - \frac{1}{2} \log \frac{\pi^2}{2} + G_0 \left(\frac{z}{2\pi} \right) \right), \quad (\text{A.5})$$

$$F_1(z; \infty) = \frac{\pi}{6} \left(\frac{1}{12} - G_1 \left(\frac{z}{2\pi} \right) \right) - \frac{z}{16} + \frac{z^4}{192\pi^3} H_1 \left(\frac{z}{2\pi} \right) - \frac{z^2}{16\pi} \left[\gamma_E - \frac{1}{2} \log \frac{\pi^2}{2} + \frac{2}{3} G_0 \left(\frac{z}{2\pi} \right) - \frac{1}{3} \right]. \quad (\text{A.6})$$

We will also need the asymptotic expansion for $z \rightarrow 0$. We have

$$F_0(z; \infty) = \frac{1}{2z} + \bar{F}_{00} + O(z^2) \quad (\text{A.7})$$

with

$$\bar{F}_{00} = \frac{1}{2\pi} \left(\gamma_E - \log \pi + \frac{1}{2} \log 2 \right), \quad (\text{A.8})$$

where $\gamma_E \approx 0.577215664902$ is Euler constant.

A.2 Computation of the FSS functions

In this Appendix we will compute the FSS functions and their leading corrections in the large- N limit for the theory defined by the action (3.1). We will follow closely the strategy of Ref. [48] to which we refer for the derivation of the basic results.

We will consider a square lattice of size $L \times T$. The FSS limit corresponds to $\beta \rightarrow \infty$, $L, T \rightarrow \infty$ with $L/T \equiv \rho$ and $m_{L,T}L \equiv z$ fixed.

The first step is the derivation of the asymptotic expression for $\omega_{L,T}$. From the gap equations (3.5) and (3.6) we obtain

$$-\frac{1}{2\alpha_3}\omega_{L,T} = \frac{\frac{1}{LT} \sum_p \frac{\hat{K}(p)}{\hat{w}(p; \omega_{L,T}) + m_{L,T}^2}}{\frac{1}{LT} \sum_p \frac{1}{\hat{w}(p; \omega_{L,T}) + m_{L,T}^2}}. \quad (\text{A.9})$$

From this equation we immediately see that, for $m_{L,T} \rightarrow 0$, the r.h.s. goes to zero for any L, T , including $L, T = \infty$. Therefore in the FSS limit $\omega_{L,T} \rightarrow 0$. Now, at least for $\omega_{L,T}$ sufficiently small, $\hat{w}(p; \omega_{L,T}) \geq 0$ everywhere since $w(p) \geq 0$; moreover $\hat{w}(p; \omega_{L,T})$ vanishes only for $p = 0$ in the Brillouin zone. Therefore, we can use the results of Ref. [48] and we can write

$$\omega_{L,T} = \frac{-2\alpha_3 \Xi_1(\omega_{L,T})}{\frac{1}{2\pi} \log L + F_0(z; \rho) + \Lambda_0(\omega_{L,T})} + O\left(\frac{\log L}{L^2}\right), \quad (\text{A.10})$$

where

$$\Lambda_0(\omega) = \int \frac{d^2p}{(2\pi)^2} \left(\frac{1}{\hat{w}(p; \omega)} - \frac{1}{\hat{p}^2} \right), \quad (\text{A.11})$$

$$\Xi_1(\omega) = \int \frac{d^2p}{(2\pi)^2} \frac{\hat{K}(p)}{\hat{w}(p; \omega)}, \quad (\text{A.12})$$

and $F_0(z; \rho)$ is defined in Eq. (A.5).

Eq. (A.10) shows that $\omega_{L,T}$ goes to zero in the FSS limit logarithmically and that it admits an expansion in powers of $1/\log L$. Explicitly we have

$$\omega_{L,T} = -\frac{4\pi\alpha_3\Xi_1(0)}{\log L} \left[1 + \frac{2\pi}{\log L} (-2\alpha_3\Xi_1(0) + 2\alpha_3\Xi_2(0) - F_0(z; \rho) - \Lambda_0(0)) \right] + O(\log^{-3} L), \quad (\text{A.13})$$

where

$$\Xi_2(\omega) = \int \frac{d^2p}{(2\pi)^2} \frac{\hat{K}(p)^2}{\hat{w}(p; \omega)^2}. \quad (\text{A.14})$$

Eq. (A.10) defines $\omega_{L,T}$ implicitly as a function of z , L , and ρ , and it should be solved exactly if we want to obtain the corrections to FSS up to terms of order $\log^2 L/L^4$. In the following we will obtain the corrections to FSS parametrized in terms of z and $\omega_{L,T}$; it is understood that $\omega_{L,T}$, for each z, L and ρ , is the solution of Eq. (A.10).

Let us now go back discussing the validity of Eq. (A.10). As already mentioned above, it is valid only for those values of $\omega_{L,T}$ such that $\hat{w}(p; \omega) \geq 0$. A second limitation derives from the asymptotic expansion of the denominator in the r.h.s. Indeed, if $\hat{w}(p; \omega) \geq 0$, the sum $\sum_p (\hat{w}(p; \omega) + m_{L,T}^2)^{-1}$ is always positive. On the other hand the asymptotic expansion is negative for large values of z . In particular, for each L and $\omega_{L,T}$ there is a unique value $z_c(L, \omega_{L,T})$ such that

$$\frac{1}{2\pi} \log L + F_0(z_c(L, \omega_{L,T}); \rho) + \Lambda_0(\omega_{L,T}) = 0. \quad (\text{A.15})$$

It is easy to check, using the results of Ref. [48], that the asymptotic expansion makes sense only for $z \ll z_c(L, \omega_{L,T})$ and that $z_c(L, \omega_{L,T})$ behaves as L for $L \rightarrow \infty$. In other words the asymptotic expansion of the lattice sum in powers of $1/L^2$ is not uniform in z : the error increases as $z \rightarrow \infty$. This fact is not unexpected. Indeed since for $L \rightarrow \infty$ we find $z_c(L, \omega_{L,T}) \sim L$, our discussion tells us that the expansion is valid only for $L \gg z$, i.e. for $m_{L,T} \ll 1$, that is when the correlation length is much larger than the lattice spacing. In Fig. 4 we report $\omega_{L,T}$ for two different values of L and $\rho = \infty$. The non-uniformity is clearly evident: the expansion worsens as $z \rightarrow \infty$ at L fixed.

A second important fact that is evident in Eq. (A.10) is that the perturbative (PT) limit $z \rightarrow 0$ at fixed L followed by the limit $L \rightarrow \infty$ does not commute with the FSS limit.

Let us consider for simplicity the strip case $\rho = \infty$ and use the asymptotic expansion (A.7). Then, in the perturbative limit, we obtain

$$\omega_{L,\infty} = -4\alpha_3 \Xi_1(0) z \left[1 - \frac{z}{\pi} (\log L + c_\omega) \right] + O(z^3 \log^2 L), \quad (\text{A.16})$$

with

$$c_\omega = 4\pi\alpha_3 [\Xi_1(0) - \Xi_2(0)] + 2\pi\bar{F}_{00} + 2\pi\Lambda_0(0). \quad (\text{A.17})$$

In the PT limit $\omega_{L,\infty}$ has an expansion in powers of z such that the coefficient of z^n is of order $(\log L)^{n-1}$. This expansion is clearly different from the expansion (A.13), that, for $z \rightarrow 0$, becomes:

$$\omega_{L,T} = \frac{-4\pi\alpha_3 \Xi_1(0)}{\log L} \left[1 - \frac{\pi}{z \log L} (1 + O(z)) + O(\log^{-2} L) \right]. \quad (\text{A.18})$$

In the FSS limit we have a different expansion in powers of $1/\log L$ with coefficients that diverge for $z \rightarrow 0$.

The next step in the derivation consists in obtaining the relation between $\omega_{L,T}$ and ω_∞ . Starting from the second gap equation (3.6) we have

$$\frac{(1 + \omega_{L,T})\omega_{L,T}}{(1 + \omega_\infty)\omega_\infty} \int \frac{d^2 p}{(2\pi)^2} \frac{\hat{K}(p)}{\hat{w}(p; \omega_\infty) + m_\infty^2} = \frac{1}{LT} \sum_p \frac{\hat{K}(p)}{\hat{w}(p; \omega_{L,T}) + m_{L,T}^2}. \quad (\text{A.19})$$

In the FSS limit, assuming always $\omega_{L,T}$ and ω_∞ small enough so that $\hat{w}(p; \omega) \geq 0$, using the results of Ref. [48], it is easy to compute

$$\frac{1}{LT} \sum_p \frac{\hat{K}(p)}{\hat{w}(p; \omega_{L,T}) + m_{L,T}^2} = \Xi_1(\omega_{L,T}) - m_{L,T}^2 \left(\frac{1}{2\pi} \log L + F_0(z; \rho) + \Xi_3(\omega_{L,T}) \right), \quad (\text{A.20})$$

$$\int \frac{d^2 p}{(2\pi)^2} \frac{\hat{K}(p)}{\hat{w}(p; \omega_\infty) + m_\infty^2} = \Xi_1(\omega_\infty) - m_\infty^2 \left(-\frac{1}{4\pi} \log \frac{m_\infty^2}{32} + \Xi_3(\omega_\infty) \right), \quad (\text{A.21})$$

with corrections of order $m_{L,T}^4 \log m_{L,T}$ and $m_\infty^4 \log m_\infty$ respectively. Here

$$\Xi_3(\omega) = \int \frac{d^2 p}{(2\pi)^2} \left(\frac{\hat{K}(p)}{\hat{w}(p; \omega)^2} - \frac{1}{\hat{p}^2} \right). \quad (\text{A.22})$$

Using Eq. (A.19) we obtain

$$\omega_\infty = \omega_{L,T} \left(1 + \Delta_\omega(z, \omega_{L,T}; \rho; L) \frac{1}{L^2} + O(\log^2 L/L^4) \right), \quad (\text{A.23})$$

where

$$\Delta_\omega(z, \omega; \rho; L) = \frac{1 + \omega}{(1 + \omega)\Xi_1(\omega) + \omega\Xi_2(\omega)} (z^2 - 32e^{-4\pi F_0(z;\rho)}) \left(\frac{1}{2\pi} \log L + F_0(z; \rho) + \Xi_3(\omega) \right). \quad (\text{A.24})$$

In the calculation of this expression we have already used the FSS result for $m_\infty^2/m_{L,T}^2$ that will be derived in the following. The function $\Delta_\omega(z, \omega; \rho; L)$ scales as $\log L$ for $L \rightarrow \infty$ and it has an expansion in powers of $1/\log L$. Explicitly

$$\Delta_\omega(z, \omega_{L,T}; \rho; L) = \sum_{k=-1}^{\infty} \frac{\delta_{\omega,k}(z; \rho)}{\log^k L}. \quad (\text{A.25})$$

The first coefficients are

$$\delta_{\omega,-1}(z; \rho) = \frac{1}{2\pi\Xi_1(0)} (z^2 - 32e^{-4\pi F_0(z;\rho)}), \quad (\text{A.26})$$

$$\delta_{\omega,0}(z; \rho) = \frac{1}{\Xi_1(0)} (z^2 - 32e^{-4\pi F_0(z;\rho)}) [2\alpha_3\Xi_1(0) + F_0(z; \rho) + \Xi_3(0)]. \quad (\text{A.27})$$

Finally let us compute the corrections to FSS for the ratio $m_\infty^2/m_{L,T}^2$. Using Eq. (3.5) we obtain

$$\frac{1}{1 + \omega_\infty} \int \frac{d^2p}{(2\pi)^2} \frac{1}{\hat{w}(p; \omega_\infty) + m_\infty^2} = \frac{1}{1 + \omega_{L,T}} \frac{1}{LT} \sum_p \frac{1}{\hat{w}(p; \omega_{L,T}) + m_{L,T}^2}. \quad (\text{A.28})$$

Using the results of Ref. [48] and Eq. (A.23), we obtain

$$\frac{m_\infty^2}{m_{L,T}^2} = f_m(z; \rho) \left(1 + \Delta_m(z, \omega_{L,T}; \rho; L) \frac{1}{L^2} + O(\log^2 L/L^4) \right) \quad (\text{A.29})$$

where

$$f_m(z; \rho) = \frac{32}{z^2} e^{-4\pi F_0(z;\rho)}, \quad (\text{A.30})$$

and

$$\begin{aligned} \Delta_m(z, \omega_{L,T}; \rho; L) &= \frac{1}{4} (12\hat{\alpha}_1 + 16\hat{\alpha}_2 - 1) (32e^{-4\pi F_0(z;\rho)} - z^2) \log L + \\ &16\pi (12\hat{\alpha}_1 + 16\hat{\alpha}_2 - 1) F_0(z; \rho) e^{-4\pi F_0(z;\rho)} \\ &- 4(8\hat{\alpha}_1 + 8\hat{\alpha}_2 - 1) e^{-4\pi F_0(z;\rho)} - 4\pi (\mathcal{F}_1(z, \omega_{L,T}; \rho) + 32e^{-4\pi F_0(z;\rho)} \Lambda_1(\omega_{L,T})) \\ &- \frac{4\pi\omega_{L,T}}{1 + \omega_{L,T}} \left(\frac{1}{2\pi} \log L + F_0(z; \rho) + \Xi_3(\omega_{L,T}) \right) \Delta_\omega(z, \omega_{L,T}; \rho; L). \end{aligned} \quad (\text{A.31})$$

Here

$$\mathcal{F}_1(z, \omega; \rho) = (1 - 12\hat{\alpha}_1)F_1(z; \rho) + z^2 \left(\frac{\hat{\alpha}_1}{8\pi} - \Lambda_1(\omega) \right) + 2\hat{\alpha}_2 z^2 F_0(z; \rho) + \frac{\hat{\alpha}_2}{2} z^3 \frac{\partial F_0}{\partial z}(z; \rho), \quad (\text{A.32})$$

$$\Lambda_1(\omega) = \int \frac{d^2 p}{(2\pi)^2} \left(\frac{1}{\hat{w}(p; \omega)^2} - \frac{1}{(\hat{p}^2)^2} + \frac{2}{(\hat{p}^2)^3} \left(\hat{\alpha}_1 \sum_{\mu} \hat{p}_{\mu}^4 + \hat{\alpha}_2 (\hat{p}^2)^2 \right) \right). \quad (\text{A.33})$$

The variables $\hat{\alpha}_1$ and $\hat{\alpha}_2$ are functions of ω defined by the asymptotic expansion for $p \rightarrow 0$

$$\hat{w}(p; \omega) = \hat{p}^2 + \hat{\alpha}_1 \sum_{\mu} \hat{p}_{\mu}^4 + \hat{\alpha}_2 (\hat{p}^2)^2 + O(p^6). \quad (\text{A.34})$$

The function $\Delta_m(z, \omega; \rho; L)$ scales as $\log L$ for $L \rightarrow \infty$ and it has an expansion in powers of $1/\log L$. Explicitly

$$\Delta_m(z, \omega_{L,T}; \rho; L) = \sum_{k=-1}^{\infty} \frac{\delta_{m,k}(z; \rho)}{\log^k L}. \quad (\text{A.35})$$

The first coefficients are

$$\delta_{m,-1}(z; \rho) = -\frac{1}{4}(12\alpha_1 + 16\alpha_2 - 16\alpha_3 - 1) (z^2 - 32e^{-4\pi F_0(z; \rho)}) \quad (\text{A.36})$$

$$\delta_{m,0}(z; \rho) = -\frac{\pi^2}{18}(1 - 12\alpha_1) + \frac{\pi z}{4} (1 - 12\alpha_1 - 12\alpha_2 + 16\alpha_3) + O(z^2). \quad (\text{A.37})$$

One immediately sees that if the action is tree-level improved $\delta_{m,-1}(z; \rho) = 0$. The next coefficient $\delta_{m,0}(z; \rho)$ instead does not vanish in general. In Fig. 5 we report the function $\Delta_m(z, \omega_{L,T}; \rho; L)$ for $\rho = \infty$ together with the exact deviations from finite-size scaling. Notice that for $L = 10$ the higher-order terms in $1/L$ behaving as $\log L/L^4$ still play an important role for $z \approx 2 - 10$, while they are negligible for $L = 30$.

Since our class of actions for $\alpha_3 \neq 0$ is only on-shell improved, we expect to find an improved behaviour only in on-shell quantities. On the strip ($\rho = \infty$) let us determine the FSS behaviour of the mass gap $\mu(L)$. In the FSS limit with $L\mu(L) \equiv x$ fixed we have

$$\frac{\mu(\infty)^2}{\mu(L)^2} = f_{\mu}(x) \left(1 + \Delta_{\mu}(x, \omega_{L,\infty}; L) \frac{1}{L^2} + O(L^{-4} \log^2 L) \right) \quad (\text{A.38})$$

where $f_{\mu}(x) = f_m(x)$ and

$$\begin{aligned} \Delta_{\mu}(x, \omega; L) &= \Delta_m(x, \omega; \infty; L) + \frac{8}{3}(12\hat{\alpha}_1 + 12\hat{\alpha}_2 - 1)e^{-4\pi F_0(x; \infty)} + \\ &+ (12\hat{\alpha}_1 + 12\hat{\alpha}_2 - 1) \frac{\pi x^3}{6} \frac{\partial F_0(x; \infty)}{\partial x} \end{aligned} \quad (\text{A.39})$$

For $L \rightarrow \infty$, $\Delta_{\mu}(x, \omega; L)$ has an expansion in powers of $1/\log L$:

$$\Delta_{\mu}(x, \omega_{L,T}; L) = \sum_{k=-1}^{\infty} \frac{\delta_{\mu,k}(x)}{\log^k L}. \quad (\text{A.40})$$

It is easy to see that $\delta_{\mu,-1}(x) = \delta_{m,-1}(x; \infty)$. Therefore the leading term vanishes for tree-level improved actions. If $\alpha_1 = \frac{1}{12}$ and $\alpha_2 = \alpha_3$ we have

$$\delta_{\mu,0}(x) = \left\{ 8\pi\alpha_2 [\Lambda_0(0) - 2\alpha_2 \Xi_1(0) - 2\Xi_2(0) - 2\Xi_3(0)] - 4\pi \left[\Lambda_1(0) - \frac{1}{96\pi} \right] - 4\pi\alpha_2 \left[3 \left(\beta_1 - \frac{1}{12} \right) + 4(\beta_2 - \alpha_2) \right] \Xi_1(0) \right\} (32e^{-4\pi F_0(x;\rho)} - x^2), \quad (\text{A.41})$$

$$\delta_{\mu,1}(x) = -4\pi\alpha_3 \Xi_1(0) \left[\frac{2\pi}{3} \left(\beta_1 - \frac{1}{12} \right) - x \left(\beta_1 - \frac{1}{12} - 32\pi^2\alpha_3 \right) + O(x^2) \right], \quad (\text{A.42})$$

where β_1 and β_2 are defined from

$$K(p) = \hat{p}^2 + \beta_1 \hat{p}^4 + \beta_2 (\hat{p}^2)^2 + O(p^6). \quad (\text{A.43})$$

From Eq. (A.41) we immediately see that it is possible to choose $w(p)$ and $K(p)$ in such a way that $\delta_{\mu,0}(x) = 0$. Actions satisfying this condition are one-loop on-shell improved. On the other hand, from Eq. (A.42), one immediately convinces oneself that $\delta_{\mu,1}(x)$ never vanishes unless $\alpha_3 = 0$. In other words, actions of the form (3.1) with $\alpha_3 \neq 0$ cannot be two-loop improved. This is not unexpected since six-spin couplings are needed for two-loop improvement.

B Perturbative computation of the mass gap for spatial momentum $p \neq 0$

In this Appendix we will compute the mass gap for states with spatial momentum p for the most general action with two-spin and four-spin couplings:

$$S(\boldsymbol{\sigma}) = \frac{1}{2} \sum_{x,y} w_{xy} \boldsymbol{\sigma}_x \cdot \boldsymbol{\sigma}_y + \sum_{x_1 x_2 x_3 x_4} c_{x_1 x_2; x_3 x_4} (\boldsymbol{\sigma}_{x_1} \cdot \boldsymbol{\sigma}_{x_2} - 1)(\boldsymbol{\sigma}_{x_3} \cdot \boldsymbol{\sigma}_{x_4} - 1). \quad (\text{B.1})$$

Notice that the couplings $c_{x_1 x_2; x_3 x_4}$ are well defined only for $x_1 \neq x_2$ and $x_3 \neq x_4$. This action reduces to (3.1) if

$$c_{x_1 x_2; x_3 x_4} = -\frac{\alpha_3}{8} K_{x_1 x_2} K_{x_3 x_4} (\delta_{x_1 x_3} + \delta_{x_2 x_3} + \delta_{x_1 x_4} + \delta_{x_2 x_4}). \quad (\text{B.2})$$

We introduce the Fourier transform

$$c(p; q, k) \equiv \sum_{x_2 x_3 x_4} c_{x_1 x_2; x_3 x_4} e^{i\frac{p}{2}(x_1+x_2-x_3-x_4)} e^{iq(x_1-x_2)} e^{ik(x_3-x_4)}, \quad (\text{B.3})$$

and define

$$C(p; q, k) \equiv c(p; q, k) - c(p; p/2, k) - c(p; q, p/2) + c(p; p/2, p/2), \quad (\text{B.4})$$

$$f(p, q) \equiv C \left(p+q; \frac{p-q}{2}, \frac{p-q}{2} \right). \quad (\text{B.5})$$

For $p, q, k \rightarrow 0$, keeping into account the lattice symmetries, we have

$$\begin{aligned}
C(p; q, k) &= \frac{1}{16}(\alpha + \beta)(p^2)^2 + \frac{1}{16}\gamma \sum_{\mu} p_{\mu}^4 - \frac{1}{4}\alpha p^2(q^2 + k^2) - \\
&\quad - \frac{1}{4}\beta [(p \cdot q)^2 + (p \cdot k)^2] - \frac{1}{4}\gamma \sum_{\mu} (p_{\mu}^2 q_{\mu}^2 + p_{\mu}^2 k_{\mu}^2) + \\
&\quad + \alpha q^2 k^2 + \beta (q \cdot k)^2 + \gamma \sum_{\mu} q_{\mu}^2 k_{\mu}^2 + O(p^6, p^4 q^2, \dots)
\end{aligned} \tag{B.6}$$

$$f(p, q) = \alpha(p \cdot q)^2 + \frac{\beta}{2} [(p \cdot q)^2 + p^2 q^2] + \gamma \sum_{\mu} p_{\mu}^2 q_{\mu}^2 + O(p^6, p^4 q^2, \dots), \tag{B.7}$$

where α, β and γ are free parameters. If $c_{x_1 x_2; x_3 x_4}$ is given by Eq. (B.2), then $\beta = \gamma = 0$ and $\alpha = -\alpha_3/2$. The general conditions that make the action (B.1) tree-level on-shell improved have been discussed in Ref. [10]. The two-point function is improved if $\alpha_1 = 1/12$, while improvement of the four-point function gives

$$\alpha = -\frac{1}{2}\alpha_2, \quad \beta = \gamma = 0. \tag{B.8}$$

Let us now compute the mass gap. Explicitly we consider

$$G(t; \bar{p}) = \frac{1}{L} \sum_{x_1, x_2} \langle \sigma_{0, x_1} \cdot \sigma_{t, x_2} \rangle e^{i\bar{p}(x_2 - x_1)} \tag{B.9}$$

on a strip $\infty \times L$ with periodic boundary conditions in the spatial direction. For large $|t|$ we have

$$G(t; \bar{p}) \sim e^{-|t|\omega(\bar{p})}. \tag{B.10}$$

The calculation at one loop for $\bar{p} = 0$ is reported in Ref. [8, 55]. Here we will repeat the calculation for $\bar{p} \neq 0$. At the order we are interested in we expand

$$\omega(\bar{p}) = \omega_0(\bar{p}) + \frac{1}{\beta}\omega_1(\bar{p}) + O(\beta^{-2}). \tag{B.11}$$

The tree-level term $\omega_0(\bar{p})$ is easily computed. Indeed at tree level we obtain for $\bar{p} \neq 0$

$$G(t; \bar{p}) = \frac{N-1}{\beta} \int_{-\pi}^{\pi} \frac{dq}{2\pi} \frac{e^{iqt}}{w(q, \bar{p})}. \tag{B.12}$$

$w(q, \bar{p})$ is a sum of trigonometric functions and therefore it is analytic in the whole complex q -plane. It is then easy to compute the integral using Cauchy's theorem. For $|t| \rightarrow \infty$ we have

$$G(t; \bar{p}) = \frac{N-1}{\beta} \frac{e^{-\omega_0(\bar{p})|t|}}{D(\bar{p})}, \tag{B.13}$$

where $i\omega_0(\bar{p})$ is the zero of $w(q, \bar{p})$ with the smallest positive imaginary part² and

$$D(\bar{p}) = -i \left(\frac{\partial w(q, \bar{p})}{\partial q} \right)_{q=i\omega_0(\bar{p})}. \tag{B.14}$$

²We assume here that $\omega_0(\bar{p})$ is real. This is not generically true, although it is always verified for $\bar{p} \rightarrow 0$.

For $\bar{p} \rightarrow 0$ we have

$$\omega_0(\bar{p}) = \bar{p} + \left(\alpha_1 - \frac{1}{12}\right) \bar{p}^3 + O(\bar{p}^5), \quad (\text{B.15})$$

$$D(\bar{p}) = 2\bar{p} \left[1 - \left(\alpha_1 - \frac{1}{12}\right) \bar{p}^2 + O(\bar{p}^4)\right]. \quad (\text{B.16})$$

For tree-level on-shell improved actions we have $\alpha_1 = 1/12$. Therefore for this class of actions $O(a^2)$ corrections vanish as expected.

Let us now consider the one-loop correction. In this case one should pay special attention to the boundary conditions in the temporal direction. As usual we consider a lattice of size $L \times T$ with free boundary conditions in the temporal direction and we will use the explicit expression for the two-point function reported in [55]. $G(t; \bar{p})$ is then obtained taking the limit $T \rightarrow \infty$. For $\bar{p} \neq 0$ we obtain the final expression

$$\begin{aligned} \omega_1(\bar{p}L)L &= \frac{1}{2} + \frac{L}{D(\bar{p})} \left[\frac{1}{L} \sum_{q_1} \int \frac{dq_0}{2\pi} \frac{w(p+q) - w(p)}{w(q)} - 1 \right] + \\ &+ 4(N-1) \frac{L}{D(\bar{p})} \left[\frac{1}{L} \sum_{q_1} \int \frac{dq_0}{2\pi} \frac{1}{w(q)} C(0; p, q) \right] + \\ &+ 8 \frac{L}{D(\bar{p})} \left[\frac{1}{L} \sum_{q_1} \int \frac{dq_0}{2\pi} \frac{1}{w(q)} (f(p, q) - f(p, 0)) \right], \end{aligned} \quad (\text{B.17})$$

where in the r.h.s. $p \equiv (i\omega_0(\bar{p}), \bar{p})$. We can then expand Eq. (B.17) in powers of $1/L$ for $\bar{p} \rightarrow 0$ with $\bar{p}L$ fixed. We obtain

$$\omega_1(\bar{p})L = \frac{1}{2} + \frac{\Omega(\bar{p}L)}{L^2} + O(L^{-4}), \quad (\text{B.18})$$

where

$$\begin{aligned} \Omega(\bar{p}L) &= \frac{\pi}{12} \bar{p}L (1 - 12\alpha_1 - 8\alpha_2 - 16\alpha - 16\gamma - 8\beta) - \frac{2\pi}{3} (N-1) \bar{p}L (\beta + \gamma) - \\ &- \left(\alpha_1 - \frac{1}{12}\right) (N-1) (\bar{p}L)^3 E + (N-1) (\bar{p}L)^3 D + \\ &+ (\bar{p}L)^3 \left[A - 3B - F - 2 \left(\alpha_1 - \frac{1}{12}\right) \left(G - \frac{1}{4}C\right) \right]. \end{aligned} \quad (\text{B.19})$$

The constants A, B, C, D, E, F , and G are explicitly given by

$$A \equiv \frac{1}{48} \int \frac{d^2q}{(2\pi)^2} \frac{1}{w(q)} \sum_{\mu} \left[\frac{\partial^4 w}{\partial q_{\mu}^4}(q) - \frac{\partial^4 w}{\partial q_{\mu}^4}(0) \right], \quad (\text{B.20})$$

$$B \equiv \frac{1}{24} \int \frac{d^2q}{(2\pi)^2} \frac{1}{w(q)} \left[\frac{\partial^4 w}{\partial q_0^2 \partial q_1^2}(q) - \frac{\partial^4 w}{\partial q_0^2 \partial q_1^2}(0) \right], \quad (\text{B.21})$$

$$C \equiv \frac{1}{2} \int \frac{d^2q}{(2\pi)^2} \frac{1}{w(q)} \sum_{\mu} \left[\frac{\partial^2 w}{\partial q_{\mu}^2}(q) - \frac{\partial^2 w}{\partial q_{\mu}^2}(0) \right], \quad (\text{B.22})$$

$$D \equiv \frac{1}{6} \int \frac{d^2q}{(2\pi)^2} \frac{1}{w(q)} \left[\left. \frac{\partial^4 C}{\partial p_0^4}(0; p, q) \right|_{p=0} - 3 \left. \frac{\partial^4 C}{\partial p_0^2 \partial p_1^2}(0; p, q) \right|_{p=0} \right], \quad (\text{B.23})$$

$$E \equiv \int \frac{d^2q}{(2\pi)^2} \frac{1}{w(q)} \left[\left. \frac{\partial^2 C}{\partial p_0^2}(0; p, q) \right|_{p=0} + \left. \frac{\partial^2 C}{\partial p_1^2}(0; p, q) \right|_{p=0} \right], \quad (\text{B.24})$$

$$F \equiv -\frac{1}{3} \int \frac{d^2q}{(2\pi)^2} \frac{1}{w(q)} \left[\left. \frac{\partial^4 f}{\partial p_0^4}(p, q) \right|_{p=0} - 3 \left. \frac{\partial^4 f}{\partial p_0^2 \partial p_1^2}(p, q) \right|_{p=0} \right], \quad (\text{B.25})$$

$$G \equiv \int \frac{d^2q}{(2\pi)^2} \frac{1}{w(q)} \left[\left. \frac{\partial^2 f}{\partial p_0^2}(p, q) \right|_{p=0} + \left. \frac{\partial^2 f}{\partial p_1^2}(p, q) \right|_{p=0} \right]. \quad (\text{B.26})$$

For the action (3.1), these expressions simplify becoming

$$D = -2\alpha_3 \left(\beta_1 - \frac{1}{12} \right) \int \frac{d^2q}{(2\pi)^2} \frac{K(q)}{w(q)}, \quad (\text{B.27})$$

$$E = -2\alpha_3 \int \frac{d^2q}{(2\pi)^2} \frac{K(q)}{w(q)}, \quad (\text{B.28})$$

$$F = -\frac{3\alpha_3}{2} \int \frac{d^2q}{(2\pi)^2} \frac{1}{w(q)} \left\{ \frac{1}{4} \left[\frac{\partial^2 K}{\partial q_0^2}(q) - \frac{\partial^2 K}{\partial q_1^2}(q) \right]^2 - \left[\frac{\partial^2 K}{\partial q_0 \partial q_1} \right]^2 + \frac{1}{3} \sum_{\mu} \frac{\partial K}{\partial q_{\mu}} \frac{\partial^3 K}{\partial q_{\mu}^3} - \frac{\partial K}{\partial q_0} \frac{\partial^3 K}{\partial q_0 \partial q_1^2} - \frac{\partial K}{\partial q_1} \frac{\partial^3 K}{\partial q_1 \partial q_0^2} \right\}, \quad (\text{B.29})$$

$$G = -\frac{\alpha_3}{4} \int \frac{d^2q}{(2\pi)^2} \frac{1}{w(q)} \left[\left(\frac{\partial K}{\partial q_0}(q) \right)^2 + \left(\frac{\partial K}{\partial q_1}(q) \right)^2 \right], \quad (\text{B.30})$$

with β_1 defined in Eq. (A.43).

If the action is tree-level on-shell improved Eq. (B.19) reduces to

$$\Omega(\bar{p}L) = (\bar{p}L)^3 [(N-1)D + A - 3B - F]. \quad (\text{B.31})$$

Notice that if we require the action (B.19) to be tree-level improved to order $O(a^4)$ we obtain the additional condition $\beta_1 = 1/12$. In this case we also have $D = 0$.

Computing numerically the various integrals, we obtain for the various actions we have introduced in the text:

1. Standard action (2.3)

$$\Omega(\bar{p}L) = \frac{\pi}{12} \bar{p}L; \quad (\text{B.32})$$

2. Symanzik action (2.4)

$$\Omega(\bar{p}L) = -0.01237(\bar{p}L)^3; \quad (\text{B.33})$$

3. Diagonal action (2.5)

$$\Omega(\bar{p}L) = \frac{\pi}{18} \bar{p}L - 0.00315(\bar{p}L)^3; \quad (\text{B.34})$$

4. On-shell action (2.1)

$$\Omega(\bar{p}L) = -0.01321(\bar{p}L)^3 - 0.01604(N-1)(\bar{p}L)^3. \quad (\text{B.35})$$

In particular for $N = 3$ and $\bar{p}L = 2\pi$ we obtain in the four cases: $\Omega(2\pi) = 1.64493, -3.0698, 0.3163, -11.235$. For the first two cases we can compare with the numerical results of Ref. [10] finding good agreement.

We have also computed $\Omega(\bar{p}L)$ for the one-loop Symanzik action of Ref. [1]. In this case we should add to Eq. (B.19) the tree-level contribution of the $1/\beta$ corrections appearing in the action. As expected the sum of the two terms vanishes. We should note that this cancellation does not happen for the Symanzik action that has been used in the simulations [56] and that is therefore clearly incorrect.

C Mass gap for the perfect action

In this Appendix we want to compute the mass gap for $\bar{p} \neq 0$ at one-loop for a generic perfect action, generalizing the results of Ref. [10]. The first step consists in deriving the perfect action for $\kappa \neq 2$. For our calculation we will be only interested in the two-spin and in the four-spin couplings. We will therefore consider the generic model (B.1). With the standard parametrization $\sigma_x = (\phi_x, \sqrt{1 - \phi_x^2})$ we obtain

$$S(\phi) = \frac{1}{2} \sum_{x,y} w_{xy} \phi_x \cdot \phi_y + \sum_{x_1 x_2 x_3 x_4} \bar{c}_{x_1 x_2; x_3 x_4} (\phi_{x_1} \cdot \phi_{x_2})(\phi_{x_3} \cdot \phi_{x_4}) + \dots \quad (\text{C.1})$$

where

$$\begin{aligned} \bar{c}_{x_1 x_2; x_3 x_4} &= c_{x_1 x_2; x_3 x_4} - \delta_{x_1 x_2} \sum_z c_{x_1 z; x_3 x_4} - \delta_{x_3 x_4} \sum_z c_{x_1 x_2; x_3 z} + \\ &+ \delta_{x_1 x_2} \delta_{x_3 x_4} \sum_{zz'} c_{x_1 z; x_3 z'} + \frac{1}{8} w_{x_1 x_3} \delta_{x_1 x_2} \delta_{x_3 x_4}. \end{aligned} \quad (\text{C.2})$$

It is easy to see that $\bar{c}_{x_1 x_2; x_3 x_4}$ satisfies the constraint

$$\sum_z \bar{c}_{x_1 z; x_2 x_3} = \frac{1}{8} w_{x_1 x_2} \delta_{x_2 x_3}, \quad (\text{C.3})$$

that is related to the $O(N)$ -invariance of the theory. In other words, an action of the form (C.1) is $O(N)$ -invariant up to terms of order ϕ^6 if and only if Eq. (C.3) is satisfied.

The couplings w_{xy} and $\bar{c}_{x_1 x_2; x_3 x_4}$ are obtained requiring the action to be a fixed point of a family of renormalization-group (RG) transformations [3] labelled by a parameter κ . One finds that w_{xy} is the perfect laplacian defined in Eq. (2.7). The four-spin coupling is the fixed point of the equation

$$\bar{c}'_{z_1 z_2; z_3 z_4} = \sum_{x_1 x_2 x_3 x_4} \bar{c}_{x_1 x_2; x_3 x_4} T_{x_1 z_1} T_{x_2 z_2} T_{x_3 z_3} T_{x_4 z_4} + b_{z_1 z_2; z_3 z_4}, \quad (\text{C.4})$$

where the matrix T_{xz} is defined in Eq. (28) of Ref. [3] and called there $M(n, n_B)$. It satisfies the properties

$$\sum_x T_{xz} = 4, \quad (\text{C.5})$$

$$\sum_z T_{xz} = 1, \quad (\text{C.6})$$

$$T_{xz} = T_{x+2n, z+n}, \quad (\text{C.7})$$

$$\sum_{x_2 x_3 x_4} b_{x_1 x_2; x_3 x_4} = 0, \quad (\text{C.8})$$

where n is an arbitrary lattice vector. It is also important to notice that T_{xz} is strongly peaked around $(x - 2z)_\mu \in \{0, 1\}$ for the range of κ considered in numerical computations.

The first step in trying to solve Eq. (C.4) (more precisely the equation $\vec{c}' = \vec{c}$) is to decide whether to work in real space or in Fourier space. Since Eq. (C.4), once written in Fourier space, does not map continuous functions into continuous functions, the more convenient choice is the first one. Moreover by working in real space one can take advantage of locality.

In order to solve Eq. (C.4) one must face various technical problems. First of all the equation involves an infinite number of couplings. However, as noticed by Hasenfratz and Niedermayer [3], the relevant couplings are of short-range type unless κ is very small or very large. One can thus hope to obtain reasonable approximations if one considers truncations that involve couplings among the spins of nearby points. We have therefore considered only couplings that are defined in an $l \times l$ square (a more precise definition will be given below). Notice that, even for small l , the number of couplings turns out to be quite large. Indeed it increases roughly as $(2l + 1)^6$. In particular the number of inequivalent couplings is 51, 771, and 5329 respectively for $l = 1, 2, 3$.

To define the domain precisely, let us begin by noticing that the couplings $\bar{c}_{x_1 x_2; x_3 x_4}$ should be invariant under the group of lattice symmetries (including of course the translations) which acts on the four points $[x] \equiv (x_1, x_2; x_3, x_4)$ and under the group of permutations generated by

$$(x_1, x_2; x_3, x_4) \rightarrow (x_2, x_1; x_3, x_4) \quad (x_1, x_2; x_3, x_4) \rightarrow (x_3, x_4; x_1, x_2). \quad (\text{C.9})$$

To each set of points $[x]$ we associate the quantity $||[x]|| \equiv \max_{\mu, i} \{x_{i, \mu}\}$ and a new set of lattice points $[d] \equiv (d_1, d_2; d_3, d_4)$ that are equivalent to $[x]$ under the above symmetries and that satisfy the following two properties: (i) $d_1 = (0, 0)$; (ii) $||[d]|| \leq ||[y]||$ for all $[y]$ equivalent to $[d]$ — and therefore to $[x]$ — such that $y_1 = (0, 0)$. The truncation to the $l \times l$ square is defined by keeping all couplings $\bar{c}_{x_1 x_2; x_3 x_4}$ such that $||[d]|| \leq l$.

Because of this truncation, solving Eq. (C.4) becomes a standard linear algebra problem. Eq. (C.4) can be rewritten as

$$\bar{c}_i = \sum_{j \in \Lambda^l} \mathbb{T}_{ij} \bar{c}_j + b_i, \quad (\text{C.10})$$

where the indices i, j run over the set Λ^l of inequivalent (with respect to the above symmetries) couplings \bar{c}_i that are defined in an $l \times l$ square.

Notice a further difficulty in Eq. (C.4): in principle we should sum over x_i ranging on all \mathbb{Z}^2 . However thanks to the observation which follows Eq. (C.8), the contributions to the sum are very small unless $|x_{i\mu}| \lesssim (2l + 1)$. Practically we found $|x_{i\mu}| \leq (2l + 4)$ to be enough at our level of precision.

Now we have to solve the linear system (C.10). One could try to find the solution iterating Eq. (C.10) a sufficient number of times (after all, it is an RG transformation). Unfortunately this approach does not work: because of Eq. (C.5), \mathbb{T} has an eigenvalue equal to 256 so that the iteration of Eq. (C.10) diverges badly. This eigenvalue is associated to the operator: $\sum_{x_1 x_2 x_3 x_4} (\phi_{x_1} \cdot \phi_{x_2})(\phi_{x_3} \cdot \phi_{x_4})$ (a rather dummy one). A better approach is to solve the equation

$$(1 - \mathbb{T})\bar{c} = b, \quad (\text{C.11})$$

with a standard method (we used both LU decomposition and singular value decomposition).

The problem is now that \mathbb{T} has two unit eigenvalues³ which are associated to two marginal operators:

$$O_1 = \int dx [\phi \cdot \square \phi]^2, \quad (\text{C.12})$$

$$O_2 = \int dx (\phi^a \square \phi^b)(\phi^a \square \phi^b). \quad (\text{C.13})$$

In other words, Eq. (C.4) does not determine $\bar{c}_{x_1 x_2; x_3 x_4}$ uniquely, but there is the freedom to add two additional conditions. However there are additional constraints on $\bar{c}_{x_1 x_2; x_3 x_4}$ that follow from Eq. (C.3) and the fact that w_{xy} is given. For instance, using Eq. (C.3), and the fact that the two-spin coupling has the standard normalization $\sum_x w_{xy}(x - y)^2 = -4$, one can see that the four-spin couplings should satisfy the conditions

$$\sum_{x_2 x_3 x_4} \bar{c}_{x_1 x_2; x_3 x_4} [(x_3 - x_1)^2 + (x_4 - x_1)^2] = -1, \quad (\text{C.14})$$

$$\sum_{x_2 x_3 x_4} \bar{c}_{x_1 x_2; x_3 x_4} [2(x_3 - x_1) \cdot (x_4 - x_2)] = -1. \quad (\text{C.15})$$

One can check that Eqs. (C.14) and (C.15) are not automatically satisfied by Eq. (C.4). Therefore they provide the additional equations necessary to have a unique solution to the linear system (C.10). The solution is obtained using the singular-value decomposition method. We have verified that the solution of the equation (C.4) and of the two constraints (C.14) and (C.15) satisfies Eq. (C.3).

With this procedure we have been able to compute the couplings $\bar{c}_{x_1 x_2; x_3 x_4}$ for various values of κ and for $l = 1$ and $l = 2$. In order to use the results of appendix B we have reexpressed the integrals A , B , D , and F in terms of real-space quantities:

$$A = \frac{1}{48} \sum_x \left\{ G_{x0} w_{x0} \sum_{\mu} x_{\mu}^4 \right\}, \quad (\text{C.16})$$

³ A necessary condition for Eq. (C.11) to have solutions is that $v_i \cdot b = 0$, where v_1 and v_2 are the left eigenvectors of \mathbb{T} with eigenvalue 1. We have explicitly verified this condition.

κ	$(A - 3B)$	D		F	
		$l = 1$	$l = 2$	$l = 1$	$l = 2$
0.25	$-0.041 \cdot 10^{-3}$	$139.1 \cdot 10^{-3}$	$204.1 \cdot 10^{-3}$	$-28.79 \cdot 10^{-3}$	$-18.88 \cdot 10^{-3}$
0.5	$-0.178 \cdot 10^{-3}$	$57.82 \cdot 10^{-3}$	$72.95 \cdot 10^{-3}$	$-10.55 \cdot 10^{-3}$	$-6.711 \cdot 10^{-3}$
0.625	$-0.266 \cdot 10^{-3}$	$32.98 \cdot 10^{-3}$	$44.05 \cdot 10^{-3}$	$-3.336 \cdot 10^{-3}$	$-3.912 \cdot 10^{-3}$
0.75	$-0.364 \cdot 10^{-3}$	$25.17 \cdot 10^{-3}$	$26.18 \cdot 10^{-3}$	$-2.555 \cdot 10^{-3}$	$-2.215 \cdot 10^{-3}$
1.0	$-0.579 \cdot 10^{-3}$	$16.23 \cdot 10^{-3}$	$8.292 \cdot 10^{-3}$	$-2.299 \cdot 10^{-3}$	$-0.792 \cdot 10^{-3}$
1.5	$-1.051 \cdot 10^{-3}$	$5.579 \cdot 10^{-3}$	$-0.008 \cdot 10^{-3}$	$-1.745 \cdot 10^{-3}$	$-1.131 \cdot 10^{-3}$
2.0	$-1.541 \cdot 10^{-3}$	$1.563 \cdot 10^{-3}$	$-0.510 \cdot 10^{-3}$	$-2.387 \cdot 10^{-3}$	$-1.957 \cdot 10^{-3}$
3.0	$-2.494 \cdot 10^{-3}$	$6.609 \cdot 10^{-3}$	$-3.031 \cdot 10^{-3}$	$-8.247 \cdot 10^{-3}$	$-1.972 \cdot 10^{-3}$
4.0	$-3.363 \cdot 10^{-3}$	$24.66 \cdot 10^{-3}$	$-7.111 \cdot 10^{-3}$	$-20.99 \cdot 10^{-3}$	$-1.292 \cdot 10^{-3}$

Table 3: Results for the integrals appearing in the calculation of the mass gap for the perfect action. Here κ is the parameter appearing in the RG transformations and l refers to the domain in which the couplings are considered.

$$B = \frac{1}{24} \sum_x G_{x0} w_{x0} x_0^2 x_1^2, \quad (\text{C.17})$$

$$D = \frac{1}{6} \sum_{x_2 x_3 x_4} \left\{ c_{x_1 x_2 x_3 x_4} G_{x_3 x_4} \left[\frac{1}{2} \sum_{\mu} (x_2 - x_1)_{\mu}^4 - 3(x_2 - x_1)_0^2 (x_2 - x_1)_1^2 \right] \right\}, \quad (\text{C.18})$$

$$F = \frac{1}{3} \sum_{x_2 x_3 x_4} \left\{ c_{x_1 x_2 x_3 x_4} (G_{x_1 x_3} - G_{x_1 x_4} - G_{x_2 x_3} + G_{x_2 x_4}) \times \left[\frac{1}{2} \sum_{\mu} (x_4 - x_1)_{\mu}^4 - 3(x_4 - x_1)_0^2 (x_4 - x_1)_1^2 \right] \right\}, \quad (\text{C.19})$$

where G_{xy} is the lattice propagator, defined by $\sum_z G_{xz} w_{zy} = \delta_{xy}$. The final results are reported in Table 3.

References

- [1] K. Symanzik, in “*Mathematical problems in theoretical physics*”, R. Schrader et al. eds., (Springer, Berlin, 1982); Nucl. Phys. **B226** (1983) 187, 205.
- [2] M. Lüscher and P. Weisz, Commun. Math. Phys. **97** (1985) 59; Erratum **98** (1985) 433.
- [3] P. Hasenfratz and F. Niedermayer, Nucl. Phys. **B414** (1994) 785.
- [4] P. Hasenfratz, Nucl. Phys. B (Proc. Suppl.) **34** (1994) 3; **63** (1998) 53.
- [5] T. DeGrand, A. Hasenfratz, P. Hasenfratz, and F. Niedermayer, Nucl. Phys. **B414** (1994) 785.

- [6] W. Bietenholz and U.-J. Wiese, Nucl. Phys. **464** (1996) 319.
- [7] K. Orginos, W. Bietenholz, R. Brower, S. Chandrasekharan, and U. J. Wiese, Nucl. Phys. B (Proc. Suppl.) **63** (1998) 904.
- [8] F. Farchioni, P. Hasenfratz, F. Niedermayer, and A. Papa, Nucl. Phys. **B454** (1995) 638.
- [9] S. P. Spiegel, Phys. Lett. **B400** (1997) 352.
- [10] P. Hasenfratz and F. Niedermayer, Nucl. Phys. **B507** (1997) 399.
- [11] S. Capitani, M. Guagnelli, M. Lüscher, S. Sint, R. Sommer, P. Weisz, and H. Wittig, Nucl. Phys. B (Proc. Suppl.) **63** (1998) 153 and references therein.
- [12] R. G. Edwards, U. M. Heller, and T. R. Klassen, Nucl. Phys. B (Proc. Suppl.) **63** (1998) 847.
- [13] M. Göckeler, R. Horsley, H. Oelrich, H. Perlt, P. Rakow, G. Schierholz, and A. Schiller, Nucl. Phys. B (Proc. Suppl.) **63** (1998) 868.
- [14] C. Dawson, G. Martinelli, G. C. Rossi, C. T. Sachrajda, S. Sharpe, M. Talevi, and M. Testa, Nucl. Phys. B (Proc. Suppl.) **63** (1998) 877.
- [15] A. M. Polyakov, Phys. Lett. **B59** (1975) 79.
- [16] E. Brézin and J. Zinn-Justin, Phys. Rev. B **14** (1976) 3110.
- [17] W. A. Bardeen, B. W. Lee, and R. E. Shrock, Phys. Rev. D **14** (1976) 985.
- [18] H. E. Stanley, Phys. Rev. **176** (1968) 718; **179** (1969) 570.
- [19] P. Di Vecchia, R. Musto, F. Nicodemi, R. Pettorino, and P. Rossi, Nucl. Phys. **B235** [FS11] (1984) 478.
- [20] V. F. Müller, T. Raddatz, and W. Rühl, Nucl. Phys. **B251** [FS13] (1985) 212; *erratum* Nucl. Phys. **B259** (1985) 745.
- [21] H. Flyvbjerg, Phys. Lett. **B219** (1989) 323; H. Flyvbjerg and S. Varsted, Nucl. Phys. **B344**, (1990) 646; H. Flyvbjerg and F. Larsen, Phys. Lett. **B266** (1991) 92, 99.
- [22] P. Biscari, M. Campostrini, and P. Rossi, Phys. Lett. **B242** (1990) 225; M. Campostrini and P. Rossi, Phys. Lett. **B242** (1990) 81.
- [23] A. B. Zamolodchikov and A. B. Zamolodchikov, Nucl. Phys. **B133** (1978) 525; Ann. Phys. (N.Y.) **120** (1979) 253.
- [24] A. Polyakov and P. B. Wiegmann, Phys. Lett. **131B** (1983) 121.
- [25] P. Hasenfratz, M. Maggiore, and F. Niedermayer, Phys. Lett. **B245** (1990) 522.

- [26] P. Hasenfratz and F. Niedermayer, Phys. Lett. **B245** (1990) 529; **B268** (1991) 231.
- [27] U. Wolff, Phys. Lett. **B248** (1990) 335.
- [28] R. G. Edwards, S. J. Ferreira, J. Goodman, and A. D. Sokal, Nucl. Phys. **B380** (1992) 621.
- [29] S. Caracciolo, R. G. Edwards, A. Pelissetto, and A. D. Sokal, Phys. Rev. Lett. **75** (1995) 1891; Nucl. Phys. B (Proc. Suppl.) **42** (1995) 752.
- [30] S. Caracciolo, R. G. Edwards, T. Mendes, A. Pelissetto, and A. D. Sokal, Nucl. Phys. B (Proc. Suppl.) **47** (1996) 763.
- [31] B. Allés, A. Buonanno, and G. Cella, Nucl. Phys. **B500** (1997) 513; Nucl. Phys. B (Proc. Suppl.) **53** (1997) 677.
- [32] B. Allés, G. Cella, M. Dilaver, and Y. Gunduc, *Testing fixed points in the 2D $O(3)$ non-linear σ -model*, hep-lat/9808003.
- [33] M. Falcioni and A. Treves, Nucl. Phys. **B265** (1986) 671.
- [34] S. Caracciolo and A. Pelissetto, Nucl. Phys. **B420** (1994) 141.
- [35] S. Caracciolo and A. Pelissetto, Nucl. Phys. **B455** [FS] (1995) 619.
- [36] D.-S. Shin, *Correction to four-loop RG functions in the two-dimensional lattice $O(n)$ σ -model*, hep-lat/9810025.
- [37] S. Caracciolo and A. Pelissetto, Phys. Lett. **B402** (1997) 305.
- [38] U. Wolff, Phys. Rev. Lett. **62** (1989) 361; Nucl. Phys. **B322** (1989) 759; **B344** (1990) 581.
- [39] R. G. Edwards and A. D. Sokal, Phys. Rev. D **40** (1989) 1374.
- [40] M. Hasenbusch, Nucl. Phys. **B333** (1990) 581.
- [41] S. Caracciolo, R. G. Edwards, A. Pelissetto, and A. D. Sokal, Nucl. Phys. **B403** (1993) 475; Nucl. Phys. B (Proc. Suppl.) **20** (1991) 72; **26** (1992) 595.
- [42] A. Buonanno and G. Cella, Phys. Rev. D **51** (1995) 5865.
- [43] S. Caracciolo, A. Montanari, and A. Pelissetto, Nucl. Phys. B (Proc. Suppl.) **63** (1998) 916.
- [44] M. Lüscher, P. Weisz, and U. Wolff, Nucl. Phys. **B359** (1991) 221.
- [45] D.-S. Shin, Nucl. Phys. **B496** (1997) 408.
- [46] F. Niedermayer, Nucl. Phys. B (Proc. Suppl.) **53** (1997) 56.
- [47] T. L. Bell and K. Wilson, Phys. Rev. B **10** (1974) 3935.

- [48] S. Caracciolo and A. Pelissetto, Phys. Rev. D **58** (1998) 105007.
- [49] N. Magnoli and F. Ravanini, Z. Phys. **C34** (1987) 43.
- [50] M. Lüscher, Phys. Lett. **118B** (1982) 391.
- [51] R. H. Swendsen and J.-S. Wang, Phys. Rev. Lett. **58** (1987) 86.
- [52] R. G. Edwards and A. D. Sokal, Phys. Rev. D **38** (1988) 2009.
- [53] B. Allés, S. Caracciolo, G. Cella, M. D'Elia, A. Montanari, and A. Pelissetto, unpublished.
- [54] M. E. Fisher and M. N. Barber, Arch. Rat. Mech. Anal. **47** (1972) 205.
- [55] P. Rossi and E. Vicari, Phys. Lett. **B389** (1996) 571.
- [56] B. Berg, S. Meyer, I. Montvay, and K. Symanzik, Phys. Lett. **126B** (1983) 467.

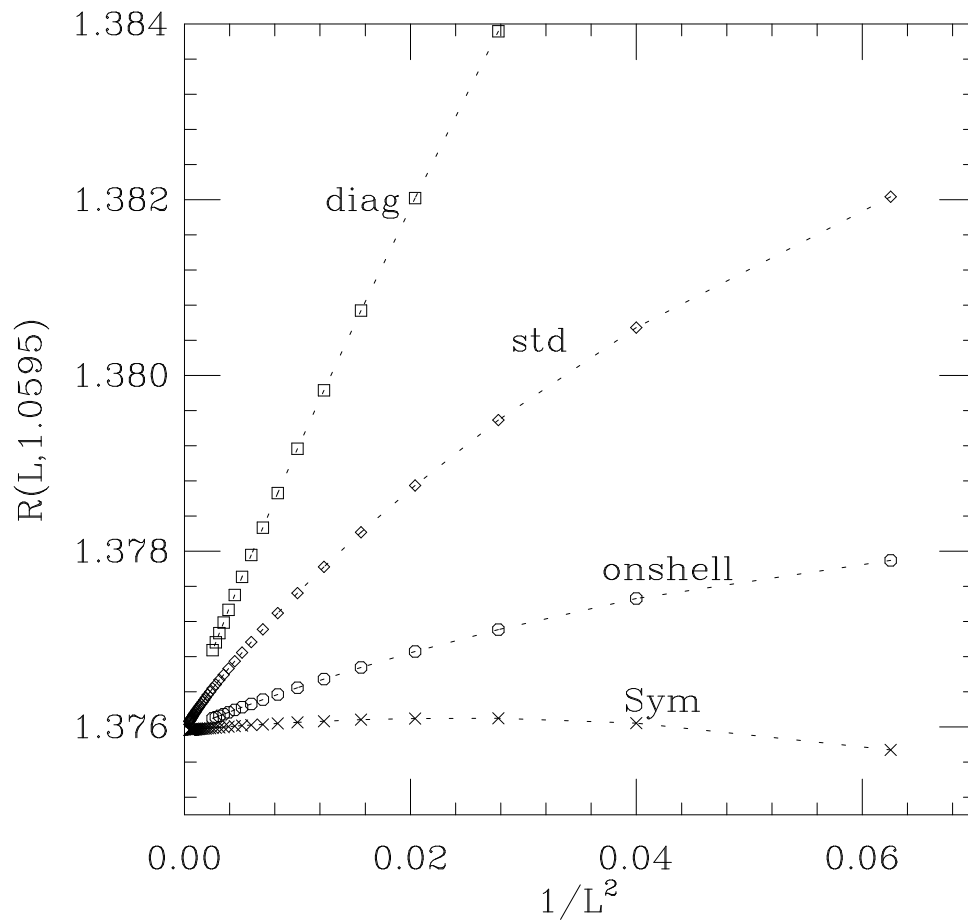


Figure 1: $\mu(2L, \beta)2L$ at $N = \infty$ with $\mu(L, \beta)L = 1.0595$ fixed for the various actions introduced in the text. “Sym”, “onshell”, “std”, “diag” refer respectively to the actions (2.4), (2.1), (2.3), (2.5).

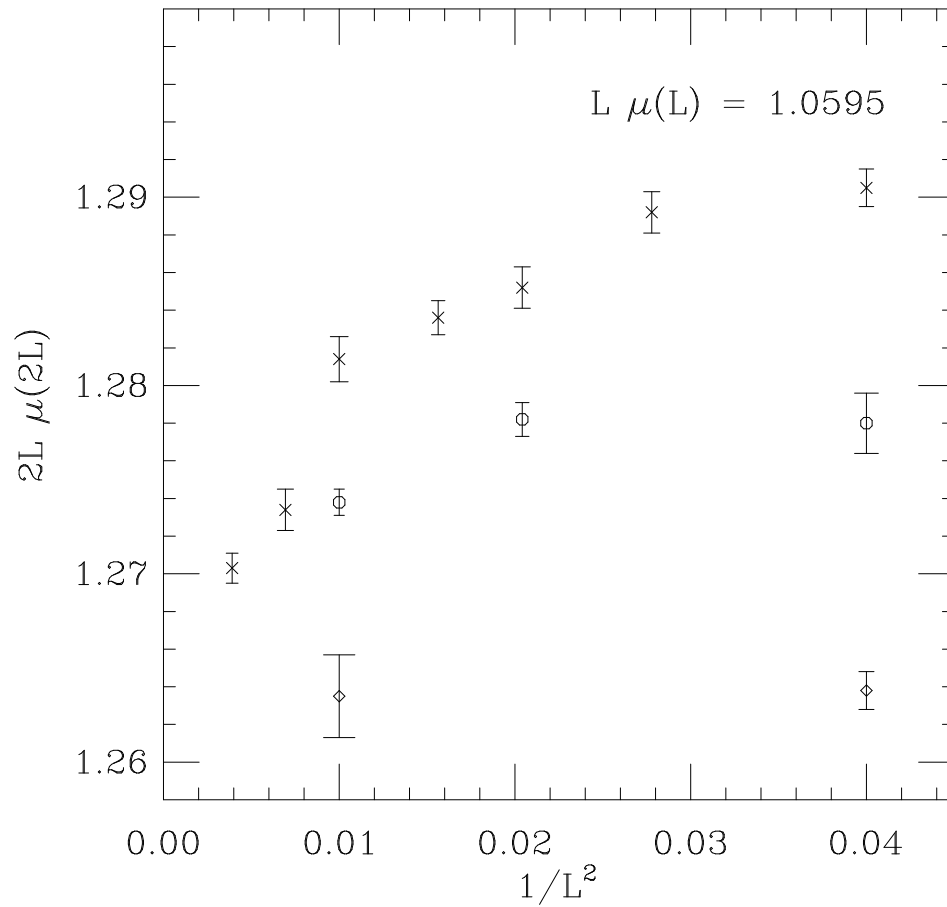


Figure 2: $\mu(2L, \beta)2L$ at $N = 3$ with $\mu(L, \beta)L = 1.0595$ fixed. Crosses refer to the standard action, circles to the on-shell tree-level improved action, and diamonds to the perfect action.

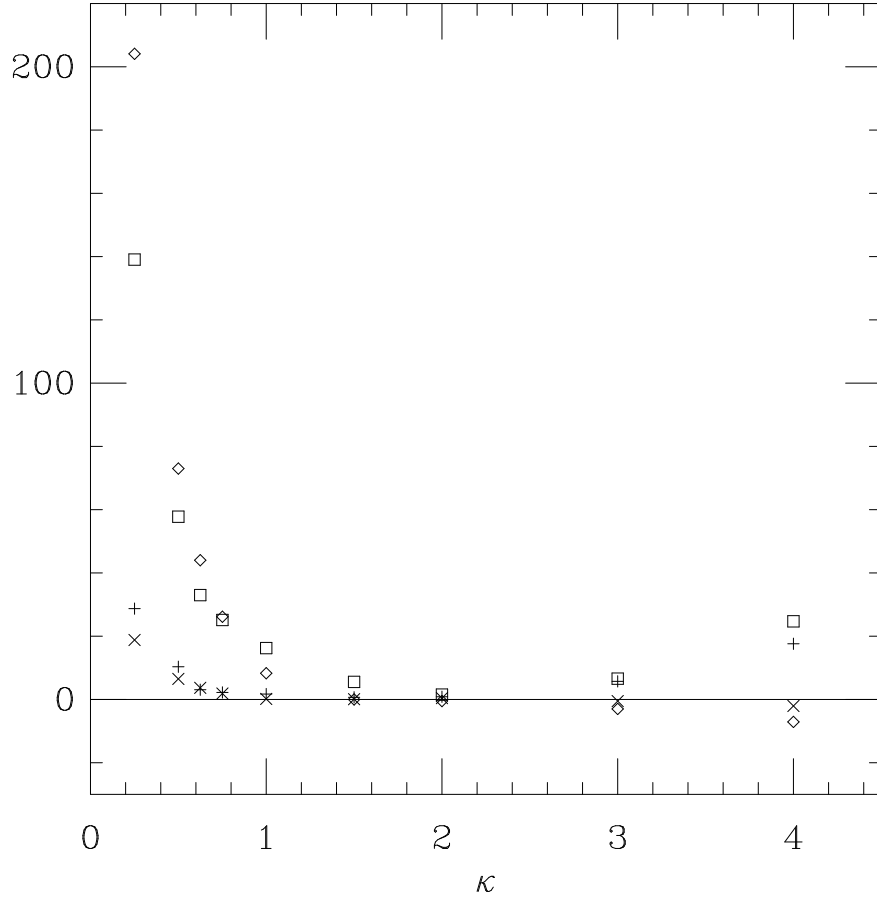


Figure 3: One-loop perturbative coefficients for the mass gap for spatial momentum $p \neq 0$. Results for various values of the renormalization-group parameter κ and truncation index l . Squares and diamonds correspond to D for $l = 1$ and $l = 2$ respectively. Pluses and crosses to the combination $A - 3B - F$ for $l = 1$ and $l = 2$ respectively. The vertical scale has been multiplied by 10^3 .

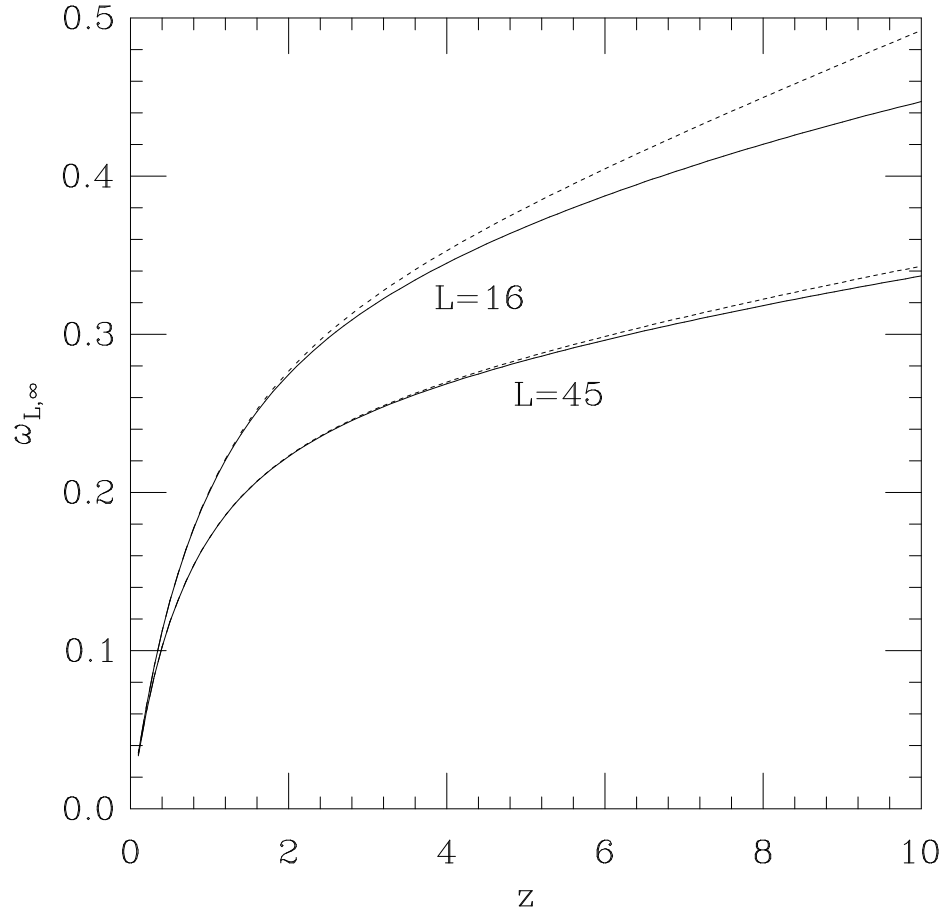


Figure 4: $\omega_{L,\infty}$ for two different values of L . The continuous line is the exact value obtained from the gap equations, while the dotted line is the solution of the equation (A.10).

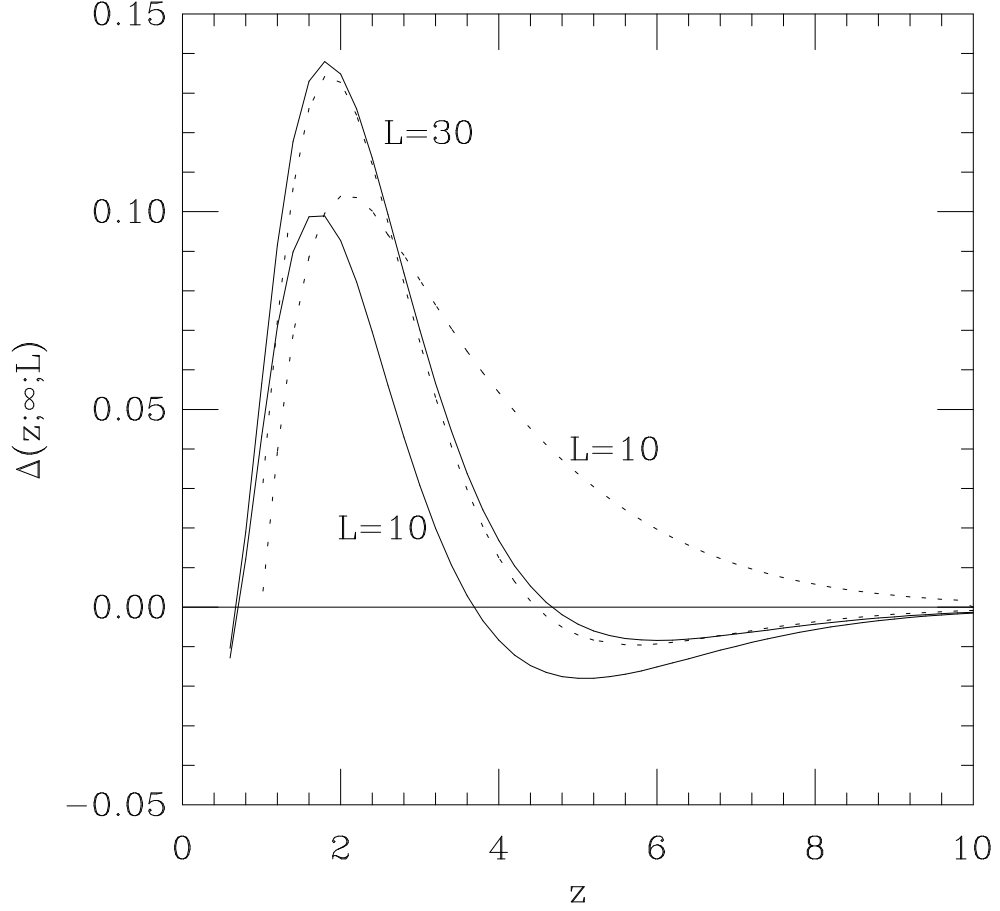


Figure 5: Scaling corrections for $\rho = \infty$ and two different values of L , $L = 10$ and $L = 30$. The full line is the exact expression $L^2(m_\infty^2/m_{L,\infty}^2 \times 1/f_m(z, \infty) - 1)$, cf. Eq. (A.29), the dashed line is the asymptotic expression $\Delta_m(z; \rho; L)$, cf. Eq. (A.31).